



1 **Extremes floods of Venice: characteristics, dynamics, past and** 2 **future evolution**

3
4
5 Piero Lionello¹, David Barriopedro², Christian Ferrarin³, Robert J. Nicholls⁵, Mirko Orlic⁴, Fabio
6 Raicich⁶, Marco Reale⁷, Georg Umgiesser³, Michalis Voudoukas⁸, Davide Zanchettin⁹

7
8 ¹University of Salento, DiSTeBA - Department of Biological and Environmental Sciences and Technologies, via per
9 Monteroni, 165, Lecce, Italy and EuroMediterranean Center on Climate Change

10 ²Instituto de Geociencias (IGEO), CSIC-UCM, C/Doctor Severo Ochoa 7, 28040 Madrid, Spain

11 ³CNR - National Research Council of Italy, ISMAR - Marine Sciences Institute, Castello 2737/F, 30122, Venezia, Italy

12 ⁴Department of Geophysics, Faculty of Science, University of Zagreb, Croatia

13 ⁵Tyndall Centre for Climate Change Research, University of East Anglia, Norwich NR4 7TJ, United Kingdom

14 ⁶CNR, Institute of Marine Sciences, AREA Science Park Q2 bldg., SS14 km 163.5, Basovizza, 34149 Trieste, Italy

15 ⁷Abdus Salam ICTP and National Institute of Oceanography and Applied Geophysics - OGS, via Beirut 2-4, Trieste, Italy

16 ⁸European Commission, Joint Research Centre (JRC), Ispra, Italy

17 ⁹University Ca' Foscari of Venice, Dept. of Environmental Sciences, Informatics and Statistics, Via Torino 155, 30172
18 Mestre, Italy

19

20 *Correspondence to:* Piero Lionello (piero.lionello@unisalento.it)

21 **Abstract**

22 Floods in the Venice city centre result from the superposition of several factors: astronomical tides, seiches and
23 atmospherically forced fluctuations, which include storm surges, meteotsunamis, and surges caused by planetary waves.
24 All these factors can contribute to positive sea-level anomalies individually and can also result in extreme sea-level events
25 when they act constructively. The largest extreme sea level events have been mostly caused by storm surges produced by
26 the Sirocco winds. This leads to a characteristic seasonal cycle, with the largest and most frequent events occurring from
27 November to March. Storm surges can be produced by cyclones whose centers are located either north or south of the
28 Alps. The most intense historical events have been produced by cyclogenesis in the western Mediterranean, to the west
29 of the main cyclogenetic area of the Mediterranean region in the Gulf of Genoa. Only a small fraction of the interannual
30 variability of extreme sea levels is described by fluctuations in the dominant patterns of atmospheric circulation variability
31 over the Euro-Atlantic sector. Therefore, decadal fluctuations of sea-level extremes remain largely unexplained. In
32 particular, the effect of the 11-year solar cycle appears to be small, non-stationary or masked by other factors. The historic
33 increase in the frequency of extreme sea levels since the mid 19th Century is explained by relative sea level rise, with no
34 long term trend in the intensity of the atmospheric forcing. Analogously, future regional relative mean sea level rise will
35 be the most important driver of increasing duration and intensity of Venice floods through this century, overwhelming
36 the small decrease in marine storminess projected during the 21 century. Consequently, the future increase of extreme sea
37 levels covers a large range, partly reflecting the highly uncertain mass contributions to future mean sea level rise from
38 the melting of Antarctica and Greenland ice-sheets, especially towards the end of the century. In conclusion, for a high
39 emission scenario the magnitude of 1-in-100 year sea level events at the North Adriatic coast is projected to increase up
40 to 65% and 160% in 2050 and 2100, respectively, with respect to the present value, and subject to continued increase



41 thereafter. Local subsidence can further contribute to the future increase of extreme sea levels. This analysis shows the
42 need for adaptive planning of coastal defenses with solutions that can be adopted to face the large range of plausible
43 future sea-level extremes.

44

45 **1. Introduction**

46 This paper reviews current understanding on the extreme water levels that are responsible for the damaging floods
47 affecting the Venice city center, such as the event on 4th November 1966, which produced estimated damages of 400
48 million euros (De Zolt *et al.*, 2006), or the event on 12 November 2019 (Cavaleri *et al.*, 2020), with estimated damage of
49 460 million euros¹ and extensive global media coverage. Future extreme floods could produce dramatic damages and
50 losses of a unique monumental and cultural heritage. Potential damages have been often linked to future relative sea level
51 rise. They have been estimated billion euros by the mid of this century if relative sea level rise (RSL) continues at the
52 observed rate for the 20th century (an unrealistic scenario based on recent trends and model projections) and reach 8 and
53 16 billion euros in severe and high-end RSL rise scenarios, respectively (Caporin and Fontini, 2016). These estimates
54 ignore adaptation options. However, they show the large exposure and the values at stake. In order to prevent damages
55 and losses of a unique monumental and cultural heritage, in 1994 the Italian government approved the construction of a
56 system of mobile barriers (MoSE, Modulo Sperimentale Elettromeccanico) to prevent the flooding of Venice during high
57 sea level events. MoSE's construction was initiated in 2003 and it has been successfully tested in October 2020. The
58 understanding of the dynamics leading to extreme water levels and the future evolution of their height and frequency is
59 of paramount importance for an accurate assessment of present and future risks. This can provide information for efficient
60 management of implemented defence systems (see also Umgiesser *et al.*, 2020, in this special issue), assessing their
61 effectiveness in the framework of the future increase of extreme sea levels and the development of new strategies to
62 cope with future scenarios (see also Zanchettin *et al.*, 2020, and Lionello *et al.*, 2020 in this special issue).

63 A clear relationship exists between the frequency of floods and RSL rise. However, this is not the only factor playing a
64 role in flooding. Section 2.1 provides a general framework for the identification of the different contributors to RSL
65 anomalies. They include a diversity of factors acting at different time scales. Extreme water levels are caused by weekly
66 to hourly atmospheric forcing, and affected by long-term (seasonal to decadal) sea level variability, which in turn depends
67 on the long-term (centennial) RSL trends (section 2.1). The timing of the surges produced by the atmospheric forcing
68 with respect to the phase of astronomical tide and free oscillations (seiches) can substantially affect the actual maximum
69 sea level (sections 2.1 and 2.2). In fact, the length of the basin and the average speed of barotropic shallow water waves
70 combine in such a way that the period of the free oscillations is close to the diurnal and semidiurnal components.
71 Therefore, the basin is close to resonant conditions and the North Adriatic has the largest tides in the Mediterranean Sea
72 (more than 1 m at the northern end of the basin), which is relevant for extreme sea levels in Venice (Figure 1). The
73 combination of all these forcings largely explains the historical floods, which are to some extent heterogeneous in terms
74 of the leading factors (see section 2.2 and appendix A1). Storm surges often yield the largest contribution to extreme sea
75 levels and in the Adriatic Sea they are caused by cyclones (as described in section 3.1). An important characteristic of the
76 Adriatic Sea (particularly its northern area) is its proximity to the cyclogenesis area in the western Mediterranean Sea,
77 where cyclones initiate their south-eastward propagation along the Mediterranean storm track and (in a small number of

¹ <https://repository.tudelft.nl/islandora/object/uuid:ea34a719-79c1-4c6e-b886-e0d92407bc9d?collection=education>



78 cases) towards central Europe (e.g., Lionello *et al.*, 2016). In autumn and winter, the area around the Adriatic Sea is
79 frequently crossed by these cyclones. The resulting south-easterly wind (Sirocco) when channeled along the main axis of
80 the basin by the action of the Apennines and Dinaric Alps is essential for producing the storm surge contribution to the
81 extreme sea levels in the northern Adriatic Sea and floods of Venice. Extreme sea levels have also been associated with
82 large-scale atmospheric variability and astronomical (solar) forcing. Available evidence of these links and their dynamics
83 are reviewed in 3.2. and 3.3.

84 A major concern is the future evolution of sea level extremes. Section 4 is devoted to past and future changes in the
85 frequency and magnitude of sea level extremes, and the relative roles of RSL rise and atmospheric forcing at different
86 time scales. Section 4 also considers the most recent estimates of the future extreme sea levels and their dependence with
87 the climate scenarios. The last section 5 provides a general assessment of the existing knowledge and indications on major
88 gaps and needs for future research.

89 2. Dynamics and characteristics of sea level evolution during an extreme flood

90 2.1. Tides, seiches and atmospherically forced sea level anomalies

91 This section describes the factors that contribute to sea level anomalies in the North Adriatic Sea: astronomical tides,
92 seiches and atmospherically forced fluctuations (which include meteotsunamis, storm surges and surges caused by
93 planetary waves) and relative sea level rise (RSLR). They are characterized by different dynamics and time scales. In
94 general, they do not have the same importance in terms of contribution to extreme sea level events, which have mostly
95 been attributed to large storm surges, whose effect was reinforced or attenuated by the remaining factors. The
96 classification of the atmospherically forced fluctuations in three categories is based on the scale of the meteorological
97 forcing process: mesoscale (tens of kilometres, minutes to hours), synoptic scale (thousands of kilometres, days) and
98 planetary scale (tens of thousands of kilometres, weeks to months). At longer time scales, inter-decadal, inter-annual and
99 seasonal (IDAS) sea level variability, natural and human induced land subsidence, and sea level rise (SLR) also contribute
100 to sea level extremes by modulating the long-term evolution of relative sea level.

101 *Astronomical tides* in the Adriatic Sea consist of two Kelvin waves oppositely travelling along the basin at semidiurnal
102 periods (Hendershott and Speranza, 1971) and of topographic waves travelling across the basin at diurnal periods
103 (Malačić, Viezzoli and Cushman-Roisi, 2000). They are adequately reproduced by a number of numerical models (e.g.
104 (Janeković and Kuzmić, 2005; Lionello, Mufato and Tomasin, 2005; Ferrarin, Maicu and Umgiesser, 2017). Diurnal and
105 semidiurnal components have their maximum amplitude at the northern shore of the basin. The semidiurnal components
106 have an amphidromic point in the centre of the Adriatic (Franco *et al.*, 1982).

107 *Seiches* in the Adriatic are standing waves with a node at the southern boundary of the basin and an antinode at the
108 northern shore. The periods of the basic modes are estimated at about 21.3 h and 10.8 h (Manca, Mosetti and Zennaro,
109 1974) and their pattern mimics the diurnal and semidiurnal tides, respectively. Seiches are commonly produced after a
110 surge, when the wind drops or switches from Sirocco (south-easterly) to Bora (north-easterly) and the water accumulation
111 in the north Adriatic ceases to be supported by the wind stress. The Adriatic seiches are damped relatively slowly, with
112 the decay time of fundamental mode amounting to 3.2 days (Cerovečki, Orlić and Hendershott, 1997), due to a weak
113 frictional dissipation inside the basin and a small energy loss to the Mediterranean Sea. There is a long tradition of
114 numerical modelling of the Adriatic seiches, e.g. (Lionello, Mufato and Tomasin, 2005), but more accurate predictions
115 of their periods and decay are still needed, e.g., (Bajo *et al.*, 2019).



116 **Storm surges** in the Adriatic have been extensively studied due to the need to forecast the floods of Venice (Robinson,
117 Tomasin and Artegiani, 1973), see Umgiesser et al., 2020 in this issue for a review. The response of the sea to air pressure
118 forcing is close to the inverted barometer effect at daily time scales, e.g., (Karabeg and Orlić, 1982). However, the surge
119 magnitude is mostly determined by the wind blowing over the shallow water areas over the North Adriatic Sea. The wind
120 contribution to sea level along the Northern coast is typically 10 times larger than the inverse barometer effect (Bargagli
121 et al., 2002; Conte and Lionello, 2013; Lionello, Conte and Reale, 2019). Surges are produced by two main winds: Sirocco
122 blowing over the whole basin and a combination of Bora over the north Adriatic and Sirocco over the south Adriatic.
123 Depending on the structure of the wind field, flooding is more pronounced along the west or the east Adriatic coast
124 (Medugorac et al., 2018).

125 **Meteotsunamis** are meteorologically-generated long ocean waves in the tsunami frequency band (Vilibić and Šepić, 2009;
126 Šepić, Vilibić and Belušić, 2009). They are generated by mesoscale air pressure disturbances that resonantly generate a
127 traveling sea level anomaly, when their speeds of propagation approach that of the shallow-water barotropic waves.
128 Meteotsunamis pose a major hazard on the eastern Adriatic coast, where their resonant periods are close to those of the
129 normal modes of the bays/harbors.

130 **Long planetary atmospheric waves** (PAW) propagate slowly and with wavelengths ranging from 6000 to 8000 km. They
131 produce a long-term meteorological forcing and eventually long-lasting sea level anomalies (**PAW surges**), which
132 establish favorable day-lasting conditions for flooding (Pasarić and Orlić, 2001).

133 The combination of storm surge, meteotsunamis and PAW surge represents the direct action of the meteorological forcing
134 on extreme sea levels and it is collectively termed **surge** in this manuscript, when no distinction is possible among the
135 different contributions.

136 The factors considered so far allow an interpretation of a typical flood (“aqua alta”, e.g. Robinson et al., 1973). When a
137 cyclone moves from western Mediterranean towards the Adriatic, low air pressure and Sirocco wind support an increase
138 of sea level in the northern Adriatic Sea and potential flooding of the area. When the cyclone leaves the Adriatic area, air
139 pressure increases while the Sirocco slackens or changes to Bora. Consequently, sea level decreases and seiches may be
140 generated. Therefore, in the Adriatic storm surges and seiches represent two distinct phases of the response to the
141 atmospheric forcing, one in which sea level rises under direct atmospheric forcing, and the other in which sea level relaxes
142 – possibly through a series of damped oscillations. If a successive storm surge develops before the attenuation of the
143 seiches induced by a previous event, a constructive or destructive superposition may occur (Bajo et al., 2019).
144 Analogously, the phase of tide during the period when the storm surge is large, can substantially increase or decrease the
145 actual sea level maximum.

146 The contribution of meteotsunamis and PAW surges to extreme sea-level events in Venice has not been thoroughly
147 investigated to date. However, the recent 12 November 2019 event uncovered their important role in flooding in Venice.
148 Therefore, in general, the hazard and probability of an extreme sea level should also include these two contributions.

149 **RSLR** represents a long-term process (see Zanchettin et al. 2020, in this special issue, for a comprehensive review of its
150 past and future evolution). It has been the dominant factor responsible for the significant increase of frequency of floods
151 of the Venice city centre (Lionello et al., 2012b). This is further modulated by IDAS sea-level variability.



152 2.2. A description of the largest past events

153 Regular instrumental observations in Venice started in 1871. Since 1919 sea-level values have been referred to the mean
154 sea level over the 1884-1909 period (central year 1897), which is usually called ‘Zero Mareografico Punta Salute’
155 (ZMPS), and referred to as relative sea level (RSL). The history of Venice tide gauges, their reference planes and the
156 related geodetic connections were described and discussed by (Dorigo, 1961a) and (Battistin and Canestrelli, 2006).
157 (Battistin and Canestrelli 2006) reviewed the observations from 1872 to 2004 and provided a complete list of high and
158 low sea-level data with the relevant primary data sources. Sea-level data are also available in the web sites of the Istituto
159 Superiore per la Protezione e la Ricerca Ambientale (ISPRA), Servizio Laguna di Venezia
160 (www.venezia.isprambiente.it), and the Centro Previsione e Segnalazione Maree of Venice municipality
161 (www.comune.venezia.it/content/centro-previsione-e-segnalazione.maree).

162 The Venice Municipality defines a high RSL event (‘aqua alta’) when relative sea level (RSL) exceeds 80 cm (above
163 ZMPS), a severe event when it exceeds 110 cm and an exceptional event when it exceeds 140 cm. Since 1872, the 140-
164 cm threshold has been exceeded during 18 events. Depending on the phase of the astronomical tide and of other factors,
165 very high RSL can or cannot correspond to very high storm surge. Table 1 list the highest RSL events² alongside the
166 contributions of various factors (in a similar way as previously done by (Orlić, 2001):

167 RELATIVE EXTREME SEA LEVEL: STORM SURGE + PAW SURGE + METEOTSUNAMI + ASTRONOMICAL
168 TIDE + SEICHE + IDAS VARIABILITY + RSLR

169 For computing the values in table 1, the long-term water level time series of Punta della Salute was processed with a tidal
170 harmonic analysis tool based on the least squares fitting (Codiga, 2011) to separate the tidal from the other contributions
171 to the total sea level. The residual sea levels were detrended for RSLR using a 10-year centered running mean. The other
172 contributions (storm surge, PAW surge, meteotsunami, local setup, seiche, IDAS variability) were estimated using digital
173 filters (low pass, band pass and high pass, as described in Ferrarin et al., 2020) in the time domain assuming Fourier
174 decomposition. The value separating storm surge and PAW surge was set to 10 days and that the corresponding value for
175 storm surge and meteotsunami (including also local set-up in the lagoon) was set to 10 hours. The separation between the
176 PAW surges and IDAS variability was achieved by applying a low pass filter with the cut-off period placed at 120 days.

177 Overall, the events listed in Table 1 agree with the ones compiled in other studies since the beginning of instrumental
178 observations (Dorigo, 1961b; Livio, 1968; Canestrelli *et al.*, 2001). The event of 4 November 1966 corresponds to both
179 the highest surge and the highest RSL. Other outstanding events are those observed on 22 December 1979 and 12
180 November 2019.

181 The event of 29 October 2018 consists of two peaks that occurred 6 hours apart, with similar RSL values (148 and 156
182 cm), but quite different phases of the astronomical tide, so that the higher water level corresponds to the lower storm
183 surge. This is the only example in 147 years of two such high RSL peaks in such a short time interval. November 2019 is
184 also peculiar because four RSL peaks with at least 140 cm height occurred on 12, 13, 15 and 17. The event of 12 November
185 2019 was particularly severe, reaching 189 cm RSL. This was the second highest ever recorded RSL. In this case the
186 storm surge was relatively modest, and the exceptional water level was caused by the superposition of PAW surges,

² Some significant surges may have been missed before 1933 due to lack of information, while all the high RSL events are available since 1872.



187 positive astronomical tide and an unprecedented contribution caused by a meteotsunami. It should be stressed that four
188 of the eight highest RSL values since 1872 were observed during the autumn seasons of 2018 and 2019.

189 The amplitude of the astronomical tide makes it an important contribution to the actual sea-level extreme and time lag
190 between the surge peak and the nearest astronomical tide maximum may make a substantial difference. Considering the
191 events described in Appendix 1, if surge and tide had peaked together, the observed RSL, based on the linear superposition
192 of the different factors (a reasonable first-order approximation for the Adriatic Sea) would have approximately been 220
193 cm, both on 4 November 1966 and 29 October 2018 (second peak), and 215 cm on 12 November 1951. Particularly, for
194 the second peak of 29 October 2018 the large magnitude of negative astronomical tide contribution has an essential role
195 to limit the impact of the event. On the contrary, the coincidence of a moderate storm surge with a preexisting seiche and
196 a high astronomical tide level produced the sixth highest level in the records.

197 In conclusion, the comparison among the different contributions in Table 1 shows that storm surge represents often the
198 largest contribution, but, in several cases, also other factors play a fundamental role. Particularly, in the case of 12
199 November 2019, the second highest ever-recorded sea level has been produced by comparable contribution from several
200 factors, with a storm surge value, which was not particularly high.

201 The meteorological and marine conditions that led to major surge events have been assessed with reanalyses and
202 dedicated model simulations, including the catastrophic storm surges of 4 November 1966 (De Zolt *et al.*, 2006; Roland
203 *et al.*, 2009; Cavaleri *et al.*, 2010), 22 December 1979 (Cavaleri *et al.*, 2010), 1 December 2008 (Medugorac, Pasarić and
204 Orlić, 2016), 1 November 2012 (Medugorac, Pasarić and Orlić, 2016), 12 November 2019 (ISPRA and CNR-ISMAR,
205 2020). Bertotti *et al.* (2011) modelled five important events that occurred between 1966 and 2008. Appendix 1 includes
206 the descriptions of major surge and RSL events and related meteorological situations.

207 The frequency of storm surges follows a strong seasonal cycle (Lionello *et al.*, 2012b). The most intense events (with
208 maxima above the 99th percentile) occur in November and December, with November concentrating the largest number
209 of intense events. However, severe events (maxima above the 80th percentile) can occur from late September to early
210 May, and, very rarely also in summer.

211 **2.3. The propagation of the sea-level signal in the interior of the lagoon**

212 North Adriatic sea-level anomalies first propagate into the lagoon through the three inlets, and then follow the tidal
213 channels. The major channels are up to 10 meters deep, and this results in a propagation speed of about 10 m/s (Umgiesser
214 *et al.*, 2004). The water then expands laterally into the shallow flats, where propagation of the wave is much slower.

215 Astronomical tides in the southern and central basins of the lagoon are slightly amplified with respect to the inlets, because
216 of resonance effects between the tide (both diurnal and semidiurnal) and the size of the basin. In the northern part of the
217 lagoon, characterized by mud flats, islands and salt marshes, dissipative processes dominate over the resonance condition,
218 so that the tidal wave shows an attenuation of about 50 % of the incoming tide (Ferrarin *et al.*, 2015). As a consequence
219 of natural and anthropogenic morphological changes that occurred in the lagoon in the last century, the amplitude of
220 major diurnal and semi-diurnal tidal constituents grew significantly, with a consequent increase in extreme high sea levels
221 in Venice (Ferrarin *et al.*, 2015).

222 The surge signal, once it has entered inside the lagoon, is able to propagate nearly without damping to the city center,
223 where sea levels are comparable to the ones close to the inlets with a typical 1 hour delay (Umgiesser *et al.*, 2004). Other
224 more remote areas of the lagoon show a higher phase shift with respect to the inlets of up to 3 hours.



225 With strong NE (Bora) or SE (Sirocco) winds, the difference between sea levels in the south and the north side of the
226 lagoon may exceed 50 cm (Mel, Carniello and D'Alpaos, 2019). The Venice city center is relatively little affected by
227 these differences, since it is close to the node of the oscillation of the water level. However, the strong setup at the southern
228 part of the lagoon can lead to flooding in the city of Chioggia.

229

230 3. Atmospheric patterns associated with extreme storm surges

231 3.1. Characteristics of cyclones producing storm surges and floods of Venice

232 The Mediterranean region is one of the areas in the Northern Hemisphere where cyclone activity is more frequent due to
233 a wide range of factors and mechanisms acting in the region which favor several cyclogenesis processes (Trigo, Davies
234 and Bigg, 1999; Lionello *et al.*, 2006a; Ulbrich, Leckebusch and Pinto, 2009; Lionello *et al.*, 2012a; Ulbrich *et al.*, 2012;
235 Lionello *et al.*, 2016). These systems are often associated with extreme weather events (Jansa *et al.*, 2001; Lionello *et al.*,
236 2006a; Toreti *et al.*, 2010; Ulbrich *et al.*, 2012; Reale and Lionello, 2013) and, more specifically, with large storm surges
237 along the Mediterranean coastline and floods of Venice (Canestrelli *et al.*, 2001; Trigo and Davies, 2002; De Zolt *et al.*,
238 2006; Lionello *et al.*, 2012b; Lionello, Conte and Reale, 2019). Cyclones produce storm surges by two mechanisms: the
239 inverse barometric effects (resulting from the decrease of atmospheric pressure during the cyclone transit over the area)
240 and the wind set-up (caused by the intense cyclonic air flow, typically Sirocco, channelled by the topography along the
241 main axis of the Adriatic Sea, which piles up water masses against the coast of the Northern Adriatic (Lionello, Conte
242 and Reale, 2019).

243 Figure 2 shows the temporal evolution of mean sea-level pressure (MSLP) fields during intense storm surge events. It is
244 a composite based on the floods with storm surge higher than 50 cm in Venice in the period 1979-2019 (Table 1) using
245 the hourly MSLP fields of ERA5 reanalysis (Hersbach *et al.*, 2020). The time lags chosen for the composites is 36, 24 ,
246 12 hours before and 12, 24 hours after the peak of the event (reported in Table 1). Figure 3 shows the same information,
247 though it is based on the remaining events in table 1, when the storm surge component did not exceed 50cm. In both
248 figures at the peak of the event, the pressure minimum is located in the Gulf of Genoa, but in figure 2 the cyclone is
249 deeper and the SLP gradient along the Adriatic Sea is larger. Further, the evolution of the cyclone before and after the
250 peak of the sea-level anomaly is different. In figure 2 cyclogenesis occurs in the western Mediterranean Sea (as noted in
251 (Lionello *et al.*, 2012b), close to the Iberian coast, as a minimum well separated from the background field. In figure 3
252 cyclogenesis occurs in the northwestern Mediterranean Sea within the flow produced by a preexisting cyclone, whose
253 center is located north of the Alps. In both figures the lee cyclogenesis processes and the generation of a secondary
254 minimum is evident (Trigo and Davies, 2002; Lionello, 2005; Lionello *et al.*, 2012b; Lionello, Conte and Reale, 2019)
255 and the pressure gradient along the Adriatic Sea intensifies and becomes almost parallel to the basin coastlines. This
256 synoptic configuration produces a decrease of the atmospheric pressure above North Italy and an increase of intensity of
257 atmospheric flow in the Adriatic Sea directed towards its northern coast, which results in the increase of sea level in
258 Venice e.g. (Lionello *et al.*, 1998).

259 Figure 4 shows the density (contours) of tracks of cyclones (measured as % relative frequency of cyclones in each cell of
260 1.5 degree) producing relative sea level higher than 110 cm ([https://www.comune.venezia.it/it/content/grafici-e-](https://www.comune.venezia.it/it/content/grafici-e-statistiche)
261 [statistiche](https://www.comune.venezia.it/it/content/grafici-e-statistiche)) in the period 1979-2019. The figures report also the tracks of all cyclones that are listed in table 1 (cyan
262 colour), of November 4th 1966 (blu line), the Vaia storm 29 October 2018 (red line) and of 12 November 2019 (green



263 line). Cyclone tracks shown in Figure 4 have been identified with an automatic detection and tracking scheme (Lionello,
264 Dalan and Elvini, 2002) to the ERA-5 MSLP fields.

265 The density of track shown in Figure 4 is characterized, in the Atlantic sector, by a peculiar north-west/south-east direction
266 which is different from the usual south-west/north-east direction observed in Atlantic (Neu *et al.*, 2013; Ulbrich *et al.*,
267 2013; Reale *et al.*, 2019). Moreover, the density of track has a maximum in the Western Mediterranean. As shown in
268 Lionello *et al.*, 2012 the tracks of cyclones producing the strongest event (Table 1 and Figure 2) have distinctive
269 characteristics with respect to the majority of cyclones crossing the Mediterranean Sea. As shown in Figure 4 many of
270 these systems enter the region from the West/South West and follow a North-East direction. On the other hand, the
271 majority of Mediterranean cyclones originate in the gulf of Genoa and follow a South-East direction (Trigo, Bigg and
272 Davies, 2002; Trigo, Davies and Bigg, 1999; Lionello *et al.*, 2006b; Ulbrich *et al.*, 2012; Lionello *et al.*, 2016). More
273 recent studies suggest that a phase-locking of the cyclone with respect to the basin seems to be critical to provide the
274 optimal conditions for surge events, with small variations in its position inducing a veering of the onshore wind and even
275 opposite responses in sea level (Lionello, Conte and Reale, 2019).

276 The diversity of triggering cyclones is also evidenced from a cluster analysis of the daily atmospheric fields associated
277 with autumn surge events in Venice (Figure 5). When all extreme surges are considered (Fig. 5a), the resulting pattern
278 resembles that of Figures 2 and 3 at the peak of the event, since the majority of extreme surge events occur in autumn
279 (see next section). However, the composite has a considerable spread (as measured by the root mean squared difference,
280 RMSD), which can be reduced by progressively discriminating types of events with a k-means analysis (Fig. 5b). Two
281 clusters bring the steepest decrease in the RMSD distribution and capture the distinction between cyclones to the north
282 and south of the Alps (Figs. 5c,d) already reported by (Lionello, 2005).

283

284 3.2. Links to large scale patterns

285 Several studies have investigated links between the main modes of atmospheric circulation variability and high surges in
286 Venice (Fagherazzi *et al.*, 2005; Lionello, 2005; Zanchettin *et al.*, 2009; Barriopedro *et al.*, 2010; Martínez-Asensio,
287 Tsimplis and Calafat, 2016).

288 The North Atlantic Oscillation (NAO) has been found to exert no significant influence on extreme surges, which are
289 linked to a different large scale circulation pattern (Lionello, 2005), being the East Atlantic (EA; (Martínez-Asensio *et al.*,
290 2014; Martínez-Asensio, Tsimplis and Calafat, 2016) or the East Atlantic Western Russia (EAWR; (Fagherazzi *et al.*,
291 2005) the teleconnection patterns that exert the largest influence on their seasonal characteristics. Another study found
292 that the negative phase of the NAO is associated with both high mean sea level and floods in Venice (Zanchettin *et al.*,
293 2009), although this signal is absent in autumn (when surges are larger). Differences in the large-scale seasonal mean
294 atmospheric circulation between active years (autumns with at least one high surge) and quiet years (autumns with no
295 high surge) have been reported (Barriopedro *et al.*, 2010). The favorable seasonal pattern for the occurrence of autumn
296 surges displays a wave train with a negative pressure center in central Europe bounded by two high pressure anomalies.

297 The aforementioned relationships are often weak, though, and hence potentially sensitive to metrics, thresholds and
298 analyzed periods. This blurred influence of teleconnection patterns is not surprising, taking into account that seasonally
299 averaged indices do not necessarily capture short-term fluctuations, and that favorable synoptic conditions (see Fig. 5)
300 might occur under different large-scale configurations. To avoid this, a Weather Regime (WR) approach is adopted herein,
301 which predefines a number of recurrent large-scale atmospheric circulation patterns and assigns each day to one of them.



302 Following (Garrido-Perez *et al.*, 2020), we considered eight WRs, which yields a fair representation of the variability all-
303 year round. Almost half of the extreme sea levels³ in Venice are associated with the Atlantic Low (AL) WR (Figure 6a),
304 whose canonical pattern (Figure 6b) strongly resembles that of Fig. 5d and of Figure 8.6 of (Lionello 2005). The remaining
305 cases (arguably many of the Mediterranean cyclones included in Fig. 5c) occur under different WRs without a clear
306 preference, although some anticyclonic WRs (e.g. the Atlantic High) are unfavorable for extreme sea levels. Despite the
307 strong association with AL on daily scales, the seasonal frequency series of AL days yields little skill on the corresponding
308 occurrence of extreme surges ($\rho=0.26$ for 1948-2018, $p<0.05$), which is similar to that obtained from other less
309 influential WRs (e.g. Zonal Regime, $\rho=0.27$; $p<0.05$). This illustrates that the interannual variability of seasonal extreme
310 sea levels cannot be well described by fluctuations in the dominant patterns of atmospheric circulation variability over
311 the Euro-Atlantic sector.

312

313 **3.3. The role of solar cycles on extreme floods**

314 Some studies have reported decadal fluctuations in the frequency of extreme surges in phase with the 11-yr solar cycle
315 during the second half of the 20th century, such that periods of high solar activity have coincided with more frequent and
316 persistent extreme surges in Venice (Tomasin, 2002; Lionello, 2005; Barriopedro *et al.*, 2010) and other Mediterranean
317 coastal stations (Martínez-Asensio, Tsimplis and Calafat, 2016). This signal results from the atmospheric forcing on sea
318 level, as revealed by hindcasts of a barotropic ocean model forced with observed atmospheric pressure and winds
319 (Martínez-Asensio, Tsimplis and Calafat, 2016).

320 An unanswered question is how such small solar forcing modulates the tropospheric circulation over the Euro-Atlantic
321 sector. Several hypotheses have been proposed, including decadal variations of the regional atmospheric circulation that
322 promote the constructive interference with the favorable pattern for the occurrence of extreme surges during periods of
323 high solar activity (Barriopedro *et al.*, 2010). Other studies claim for a solar modulation of the stratospheric polar vortex
324 and a lagged response of the NAO, e.g. (Thiéblemont *et al.*, 2015) and reference therein). However, this mechanism
325 would mainly affect the winter NAO, rather than the decadal variability of autumn extreme surges in Venice. In addition,
326 modeling studies reveal negligible impacts of the 11-yr solar cycle on the NAO and demonstrate that decadal variations
327 of the NAO can eventually vary in phase with the 11-yr solar cycle by random chance (Chiodo *et al.*, 2019). Given the
328 lack of mechanistic understanding, the null hypothesis of internal variability cannot be rejected.

329 Indeed, an updated analysis of the longest series of daily RSL in Venice (Raicich, 2015) shows that the 11-yr solar signal
330 is no longer evident in the frequency series of autumn extreme surges since the ~2000s, nor it was present before the
331 ~1950s (Figure 7 top panel). Significant correlations are limited to the period from 1970 to 2000 (Figure 7, bottom panel)
332 and give rise to strong co-variability during the second half of the 20th century, coinciding with the Grand Solar Maxima
333 covered by most studies. Further, there is no indication of the presence of a 11-year periodicity in the mean sea level and
334 its extremes (figures III.1 and III.2). Therefore, either the solar signal is non-linear, non-stationary (arguably masked by
335 other sources variability) or the decadal variability of extreme surges is due to other causes, likely internal variability. It
336 is reasonable that, superimposed on the uncontroversial increasing frequency of Venice flooding due to the mean sea-
337 level rise, large interannual-to-decadal variations will continue in the future, the causes of which are still uncertain.

³ Events with maximum sea level above the 99.5th percentile of the 1948-2018 distribution



338 **4. Past and future evolution**

339 **4.1. Past evolution and recent trends of floods and extreme sea levels**

340 (Enzi and Camuffo, 1995) presented the most complete compilation of pre-instrumental extreme sea-level events
341 observed in Venice by reviewing hundreds of historical documents, thus obtaining a sequence of over 100 events in the
342 787-1867 period. The long-term evolution has been studied by (Camuffo and Sturaro, 2004) combining information from
343 documentary sources and instrumental observations. From 1200 to 1740 the flood frequency was $<0.1 \text{ yr}^{-1}$, except for the
344 Spörer period (1500-1540), when it was 0.63 yr^{-1} . Subsequently, the frequency increased from 0.19 yr^{-1} in 1830-1930 to
345 1.97 yr^{-1} in 1965-2000.

346 Former studies of recent trends (Trigo and Davies, 2002) found that in the second half of the 20th century the local mean
347 sea-level rise compensated the decreasing frequency of storms, leading to no change in the frequency of floods. Other
348 studies, found a significant positive trend of moderate surges in Venice and Trieste during the second half of the 20th
349 century (1951-1996), that was attributed to increases in the frequency of Sirocco wind conditions over the central and
350 southern Adriatic (Pirazzoli and Alberto, 2002). A more recent study considered data in the period 1940-2007, reporting
351 a 4% reduction of all surges, but no significant increase in the frequency or intensity of the most extreme events if the
352 effect of RSLR is subtracted to the sea-level data (Lionello *et al.*, 2012b). According to (Ferrarin *et al.*, 2015), the detected
353 increase in amplitude of the tidal waves enhanced the occurrence of extreme high sea levels in Venice in the period 1940-
354 2014, while changes in storminess had no significant long-term impact. Observations made in Venice and Chioggia
355 allowed to extend the series of storm surges back to the second half of the 18th century (Raicich, 2015). For this longer
356 period, the time series of surge frequency did not exhibit a significant long-term trend, but strong inter-annual and inter-
357 decadal variability. In summary, the amount of current evidence shows that while the frequency of floods has clearly
358 increased in time, there is no clear indication of a trend in either the frequency or the severity of extreme surge events.
359 The long term increase of flood frequency is largely caused by the relative mean sea-level rise (connected to both climatic
360 change and land subsidence, see Zanchettin *et al* 2020 in this special issue).

361

362 **4.2. Future evolution of extreme sea levels**

363 Several past studies considered the future evolution of storm surges in the Adriatic Sea. A first analysis was based on a
364 doubled- CO_2 scenario and a single climate simulation (Lionello, Nizzero and Elvini, 2003). Successive studies adopted
365 the SRES scenarios and multiple simulations (Marcos *et al.*, 2011; Lionello, Galati and Elvini, 2012; Troccoli *et al.*, 2012;
366 Mel, Sterl and Lionello, 2013). The most recent studies have considered the whole Mediterranean Sea or large parts of it
367 and an ensemble of simulations (Conte and Lionello, 2013; Androulidakis *et al.*, 2015; Vousdoukas *et al.*, 2016; Lionello
368 *et al.*, 2017; Mentaschi *et al.*, 2017; Vousdoukas *et al.*, 2017; Vousdoukas *et al.*, 2018). All studies show a remarkable
369 agreement on suggesting non-significant changes or even a significant reduction of the intensity of future surges, which
370 might reach about 5% for the RCP8.5 emission scenario at the end of the 21st century. However, the future increase of
371 relative mean sea level has been shown to be the dominant factor (Lionello *et al.*, 2017; Jackson and Jevrejeva, 2016;
372 Jevrejeva *et al.*, 2016; Vousdoukas *et al.*, 2017; Vousdoukas *et al.*, 2018) and it will cause increase of frequency and
373 height of floods. Only a very low rate of future sea-level rise, such as that hypothesized in (Troccoli *et al.*, 2012), might
374 prevent future increase of floods. However, such a low future rate of rise is very unlikely (Jordà, Gomis and Marcos,
375 2012). It is lower than the global sea-level rise under the low RCP2.6 scenario in the IPCC SROCC (Oppenheimer *et al.*,
376 2019) and it would require relative sea level in Venice during the 21st century to be lower than observed during the 20th
377 century (see also Zanchettin *et al.* 2020, in this issue).



378 The future variation of amplitude of tides and surges in response to sea-level rise will depend how the coast is adapted
379 (Bamber and Aspinall, 2013) – protection versus retreat. (Lionello, Mufato and Tomasin, 2005) showed that a full
380 compensation strategy (protection), preserving the present coastline by dams, would reduce the amplitude of tides and
381 storm surges, while a no compensation strategy, allowing permanent flooding of the low coastal areas (retreat), would
382 increase the amplitude of the diurnal components and the amplitude of storm surges at the North Adriatic coast. These
383 effects are small, but not completely negligible, being about 10% for the diurnal component in case of 1-m sea-level rise.

384 Projections of extreme sea levels were produced combining dynamic simulations of all relevant components during the
385 present century, and under RCP4.5 and RCP8.5 scenarios. They include: mean sea-level rise and sea-level anomalies
386 driven by tides, surges and wind wave set-up (Vousdoukas *et al.*, 2017; Mentaschi *et al.*, 2017; Vousdoukas *et al.*, 2018).
387 MSLs were produced through a probabilistic process-based framework (Jackson and Jevrejeva, 2016; Jevrejeva *et al.*,
388 2016), incorporating the large uncertainties originating from the Greenland and Antarctic ice sheets under RCP8.5
389 (Bamber and Aspinall, 2013). Values for different return periods were estimated using non-stationary extreme value
390 statistical analysis (Mentaschi *et al.*, 2016). Here, the spatially average values along the north-west Adriatic coast (i.e.
391 from the Po delta to the Gulf of Trieste) have been extracted from the above datasets, which have pan-European or global
392 coverage.

393 The 100-year extreme sea level (100y-ESL) (Figure 8) at the North Adriatic Sea by 2050 is very likely (5-95th percentile)
394 to rise by 5 to 23 cm under the RCP4.5 moderate-emission-mitigation-policy scenario and by 17 to 62 cm under the
395 RCP8.5 high emissions scenario (Vousdoukas *et al.*, 2018). Similarly, rise to 20-38 cm and 48-175 cm, respectively, by
396 the end of the century.

397 Breaking down the contributing factors to the increase in 100y-ESLs (Figure 9), thermal expansion accounts for 45% and
398 38% (median values) of the projected rise towards the end of the century, under RCP4.5 and RCP8.5, respectively while
399 the Antarctica and Greenland ice sheet melting contribution vary from 15% to 23% (median values). However, the
400 combined contributions from ice mass-loss from glaciers, and ice-sheets in Greenland and Antarctica together, are the
401 dominant factor by 2100, contributing to 54% and 50% (median values) of the 100y-ESL increase under a moderate-
402 emission-mitigation-policy scenario (RCP4.5) and a high emissions scenario (RCP8.5), respectively.

403 The increase in 100y-ESLs corresponds to more frequent occurrence of present 100y-ESL values. By the year 2050, the
404 frequency of present-day 100-year events is projected to increase by 2 or 10 times (50 or 10 years) depending on the
405 emissions scenario. By the end of this century, events with the severity of current 1-in-100-year ‘acqua alta’ would occur
406 at least every 5 years under the RCP4.5 and more than once the RCP8.5 scenario, respectively.

407 **5. Conclusions and outlook**

408 There is a widespread view that extreme sea levels in the Venice city center are mostly caused by storm surges and that
409 the actual maximum sea level depends substantially on the timing of the storm surge peak with respect to the phase of the
410 astronomical tide. Consequently, efforts have traditionally focused on the correct simulation of the intensity, timing and
411 spatial variability of the wind (mainly the Sirocco) for the accurate reproduction of sea-level extremes. This review
412 confirms the paramount importance of storm surge, which produced the highest recorded flood (4 November 1966), but
413 also identifies other phenomena that, though they individually produce lower sea-level anomalies than storm surge, can
414 act constructively and yield extreme water levels. The event of 12 November 2019 (the second highest ever recorded
415 flood) provides a good example. Therefore, research is required on PAW and meteotsunamis, the other synoptic drivers



416 of surges, including their joint distributions, in order to better understand the likelihood of compound events as that of
417 November 2019.

418 Another poorly addressed factor is the influence of wave-set up and its effect on the sea-level anomalies inside the Venice
419 lagoon. Some studies have considered it during individual storms affecting Venice (Bertotti and Cavaleri, 1985;
420 LIONELLO, 1995; De Zolt *et al.*, 2006) and in 100y-ESL projections (Vousdoukas *et al.*, 2016; Vousdoukas *et al.*, 2017).
421 These studies show that the wave set-up contribution at the shoreline can exceed 10 cm, but the relevance for the flooding
422 of Venice city center was never analysed.

423 The long-term RSLR is modulated by sea-level variability at shorter time scales (from seasonal to decadal). Similarly,
424 the occurrence of storm surge events also displays strong interannual to decadal variability. Evidences linking this
425 variability with astronomical (e.g. the solar cycle) and climate patterns (e.g. North Hemisphere teleconnections) remain
426 elusive, from both statistical and theoretical approaches. These issues are important for the development of seasonal
427 predictions of sea-level extremes, understanding of observed trends and their attribution to long term anthropogenic
428 climate change (and local subsidence). Longer records and better understanding of the sea-level responses to atmospheric
429 forcing and remote influences would contribute to fill these knowledge gaps.

430 The synoptic conditions leading to extreme storm surges at Venice are clearly documented, as they are produced by
431 cyclogenesis occurring in the western Mediterranean Sea. There is consensus on the secondary role that the
432 meteorological forcing and marine storminess play in the long-term changes of major floods. This influence may decrease
433 further in the future with the projected attenuation of storm surges. However, the confidence on future weakening of
434 storm surges depends on the capability of climate models to correctly reproduce this process under climate change. In
435 addition, storm surges do not account for the full atmospheric forcing of extreme sea-level events. Literature on
436 projections of PAW surges and meteotsunamis is presently unavailable and progress on these factors is urgently required
437 as their changes may be different from those of storm surges. Therefore, while presently available studies agree on the
438 future attenuation of storm surges, analyses including all atmospheric forcings of extreme sea-level events are missing
439 and deserve investigation.

440 This review confirms the consensus concerning the key control of historic and future RSLR on the frequency and severity
441 of floods in Venice. Hence, understanding and predicting the future evolution of extreme sea levels in Venice depends
442 critically on the availability of RSLR projections with lower uncertainty than at present. A large fraction of such
443 uncertainty is related to the future emission scenario. Adopting a moderate-emission-mitigation-policy scenario
444 (RCP2.6), or a high emissions scenario (RCP8.5) would imply a 30% difference in the projected 100y-ESL at the end of
445 the 21st century. Another major source of uncertainty concerns the melting of ice-sheets, which accounts for the largest
446 increase of the 100y-ESL at the end of this century, particularly for a high emission scenario. Local anthropogenic and
447 long term natural subsidence can further contribute to the future increase of extreme sea levels (see Other factors, such
448 as changes in storminess or the deviation of the Mediterranean mean sea level from that of the Subpolar North Atlantic
449 (caused by steric effects and redistribution of mass within the Mediterranean Sea) appear to be less important (see
450 Zanchettin *et al.*, 2020 in this special issue).

451 Reducing uncertainty in the future projections of sea-level extremes is only one aspect of the research needed. The other
452 aspect is adaptive planning of coastal defences to consider the large uncertainty of future sea-level extremes. A moderate



453 scenario suggests a 10% and 30% increase of 100y-ESL in 2050 and 2100, respectively. A high emission scenario shows
454 a 25% increase already in 2050, reaching 65% in 2100. These ranges are further enlarged by the uncertainty in scenario
455 projections (leading to 100y-ESL increase up to 65% and a 160% in 2050 and 2100, respectively), which should be further
456 expanded to higher values including high-end RSLR scenarios (see Zanchettin et al., 2020 in this issue). The large range
457 of possible changes, especially after 2050 is not expected to be reduced substantially in the upcoming years, as it largely
458 relies on human decisions and pervasive modeling uncertainties, which limits the generation of constrained climate
459 information and poses major challenges for policy-making decisions on the development of effective adaptation
460 measurements. These results (see also Lionello et al. 2020 in this special issue) stress the need for planning and
461 implementing defense strategies of Venice that can be adapted to face the large range of plausible future sea-level
462 extremes.

463 **Acknowledgements**

464 M. Reale has been supported in this work by OGS and Cineca under HPC-TRES award number 2015-07 and by the
465 project FAIRSEA (Fisheries in the Adriatic Region - a Shared Ecosystem. Approach) funded by the 2014 - 2020 Interreg
466 V-A Italy - Croatia CBC Programme (Standard project ID 10046951). The work of M. Orlić has been supported by
467 Croatian Science Foundation under the project IP-2018-01-9849 (MAUD). Scientific activity by DZ and GU performed
468 in the Research Programme Venezia2021, with the contribution of the Provveditorato for the Public Works of Veneto,
469 Trentino Alto Adige and Friuli Venezia Giulia, provided through the concessionary of State Consorzio Venezia Nuova
470 and coordinated by CORILA. D. Barriopedro was supported by the Spanish government through the PALEOSTRAT
471 (CGL2015-69699-R) and JEDiS (RTI2018-096402-BI00) projects.
472

473 **Author contribution**

474 PL coordinated the paper. Specific contributions to the sections are as follows (LA = leading author, CA = contributing
475 author). Section 1: LA: PL; CA: RJN, DZ. Section 2: LA: MO and FR; CA: PL, GU, CF. Section 3: LA: MR and DB,
476 CA: FR and PL. Section 4: LA: MV, CA: FR, PL. Section 5: LA: PL, CA: RJN, DZ, DB. Figure 1, 2, 3 and 4 MR,
477 Figures 5 and 6 DB; figures 7 and 8 MV. Table 1: CF; table 2: FR; Appendices: AI: FR; AII: MR; AIII: DB; Figure III1
478 and III2, DB.

479

480 **Competing Interest**

481 The authors declare that they have no conflict of interest.

482

483 **6. Appendix I: Selected major events**

484 Here we present a short description of extreme sea-level events based on original reports. Each description is based on
485 the cited sources, which often include synoptic weather maps and diagrams of relevant meteorological parameters (see
486 table A.1)

487 **A1.0. 15 January 1867**

488 On 15 January 1867, that is just few years before the beginning of regular sea-level records a remarkable storm surge
489 occurred. Although no tide gauge data are available, contemporary sources reported measurements taken at local
490 hydrometers.

491 Zantedeschi (1866-67), quoting the local Civil Engineering Office (Ufficio del Genio Civile), reported that the maximum
492 observed height was 1.59 m 'above the common ordinary high water marked at the royal hydrometer in the Grand Canal'.



493 The ‘common ordinary high water’ is also known as the ‘comune marino’ (CM), that is the upper edge of the green belt
494 formed by algae on quays and walls, often indicated by an engraved horizontal mark and/or a ‘C’ (Rusconi, 1983;
495 Camuffo and Sturaro, 2004). According to Dorigo (1961a) the ZMPS is 22.46 cm below the CM of 1825, upon which
496 the tide gauge zero at S. Stefano was based. Therefore, under the hypothesis that the same CM was adopted at the royal
497 hydrometer and at S. Stefano, the maximum RSL should have been approximately 181 cm above ZMPS.

498 However, later sources gave different figures. Annali (1941) reported 132 cm above the 1825 CM, therefore the height
499 would turn out to be 154 cm (153 is reported, maybe due to rounding). Dorigo (1961) also reported 153 cm, probably
500 quoting Annali (1941).

501 If the 181-cm height was correct, the 1867 height would be the third highest RLS ever measured in Venice, not too far
502 from the 187 cm of 12 November 2019 and the 194 cm reached on 4 November 1966. Note, however, that in the 1860’s
503 the relative MSL was about 30 cm lower than at present, which makes the 1867 event very remarkable.

504 **A1.1. 16 April 1936**

505 A cyclone affected the western and central Mediterranean, with a minimum SLP around 990 hPa in the Gulf of Lions,
506 causing strong southerly winds blew over the Adriatic. In Venice wind mostly blew from the first quadrant but it veered
507 to SSW near the surge peak, with gust speed over 25 m s^{-1} ; in the meantime the SLP dropped to 990 hPa.

508 The RSL reached 147 cm; at that time it represented the second highest value ever recorded, the first having been observed
509 on 15 January 1867 (see Appendix 2). The RSL peak occurred about 2 hr after the astronomical tide maximum. The surge
510 contribution was about 94 cm.

511 **A1.2. 12 November 1951**

512 From 10 to 12 November a deep cyclone formed in the Ligurian Sea where SLP dropped from 1008 to 984 hPa. On the
513 Ionian Sea and the Balkans SLP was higher than 1012 hPa, and the strong SLP gradient induced strong southerly winds
514 over the Adriatic Sea, up to over 20 m s^{-1} in Venice. As a result, the RSL in Venice increased both because of the wind-
515 induced surge and the local IB effect. Luckily, the surge peak occurred at the astronomical tide minimum; if it had
516 occurred at the next high tide, 5 hr later, the observed RSL would have been about 65 cm higher. The RSL peak was 151
517 cm and it exceeded the official danger level of 110 cm for about 9 hr. The surge peak attained 84 cm.

518 **A1.3. 4 November 1966**

519 On 3 and 4 November 1966 the SLP field over the Mediterranean was characterized by a cyclone to the west and an
520 anticyclone to the east. The cyclone centre deepened and slowly moved from the northwest Mediterranean to northeast
521 Italy, while the zonal SLP gradient increased over the Adriatic. As a consequence, strong and persisting southerly wind
522 affected the Adriatic Sea. In Venice Sirocco speed reached 20 m s^{-1} with gusts up to 28 m s^{-1} , and the SLP dropped to 992
523 hPa.

524 The RSL height of 194 cm and the surge height of 143 cm are the highest values in the whole record. The RSL remained
525 over 110 cm for 22 hr. Economic losses for the city of about 400 hundred millions euros have been estimated.

526 Note that two elements limited the RSL peak, namely the fact that the astronomical tide was near zero at the time of the
527 maximum surge, and that in those days the Moon phase was close to last quarter, making the astronomical tide amplitude
528 relatively small, around 30 cm. Had the surge peak occurred 5 hr earlier, the RSL would have attained about 220 cm.



529 **A1.4. 22 December 1979**

530 This event was connected with a cyclone whose minimum was less than 990 hPa, that moved on 21 and 22 December
531 from the Algerian coast to the Gulf of Genoa. The combination with higher SLP over the Balkans enabled southerly wind
532 blow over the central and southern Adriatic, with gusts up to 20 m s^{-1} , while in the northern Adriatic Bora prevailed with
533 gusts over 20 m s^{-1} . The local SLP was not particularly low (1001 hPa) thus the surge was mainly attributed to wind.

534 The surge peak reached 108 cm and came 3 hr before the astronomical tide maximum: nevertheless, the RSL was
535 remarkably high, namely 166 cm which represents the third highest observed value. A RSL higher than 110 cm lasted for
536 7 hr.

537 **A1.5. 1 February 1986**

538 The synoptic situation consisted of cyclone over the western Mediterranean, this time centred in the Gulf of Lions, and
539 an anticyclone over eastern and northern Europe. A southerly wind flow affected the whole central Mediterranean,
540 including the Adriatic Sea, but a Bora component was present over the northern Adriatic. Southerly wind was particularly
541 strong in the southern Adriatic (almost 30 m s^{-1} gusts in Bari), while in Venice Bora gusts were faster than 20 m s^{-1} .

542 This event is characterised by the fourth highest RSL ever measured in Venice, that is 159 cm. The event severity was
543 the result of a moderate surge of 70 cm, that occurred just 1 hr after a 35 cm astronomical tide maximum. Overall, the
544 surge exceeded 60 cm for 15 hr.

545 **A1.6. 6 November 2000**

546 This event was caused by the combined effect of a large cyclone affecting the whole western Europe and an anticyclone
547 over eastern Europe. The lowest SLP was observed in the English Channel with values lower than 970 hPa. The eastward
548 movement of the cyclone caused the whole Adriatic to experience a remarkable SLP decrease in the 24 hr preceding the
549 surge, up to a 27-hPa drop in Venice.

550 As on 1 February 1986, during this event the storm surge and the astronomical tide maximum almost coincided. The
551 observed RSL attained 144 cm and the surge grew up to 89 cm. The RSL remained above 100 cm for over 7 hr.

552 **A1.7. 1 December 2008**

553 An intense cyclone, with strong westerly flow affected the western Mediterranean Sea. The day before the surge a small-
554 scale cyclonic circulation developed over the Gulf of Genoa and moved eastward into the River Po valley. This caused
555 surface wind over the Tyrrhenian and Adriatic Seas to veer from W to SW, then to S, intensifying in the meantime and
556 reaching the maximum intensity in the early hours of 1 December. In the afternoon, the cyclonic circulation began
557 weakening and the intensity of the associated wind in the Adriatic Sea progressively decreased.

558 From the late afternoon of 30 November to the early morning of 1 December, SLP in Venice dropped by about 13 hPa in
559 9 hr, reaching 994 hPa. The wind veered from NNE to SE around 01:30 UTC, with speed between 15 and 20 m s^{-1} for
560 the following 7-8 hr.

561 The RSL attained 156 cm, that is the fifth highest value since 1872. The maximum surge height was 61 cm and it occurred
562 less than 1 hr before the astronomical tide maximum.

563 **A1.8. 29 October 2018**

564 The event was caused by the combined action of a cyclone, centred between the Gulf of Lions and the Gulf of Genoa,
565 whose minimum SLP was lower than 985 hPa, and an anticyclone over northeastern and eastern Europe. This



566 configuration enabled strong Sirocco along the Adriatic, with speed around 15 m s^{-1} and gusts up to 25 m s^{-1} from the late
567 morning to the evening in Venice, where SLP reached a minimum of 996 hPa.

568 The strength and persistence of southerly winds caused the sea level to remain particularly high. The highest RSL was
569 reached at 13:40 UTC with 156 cm (fifth value in the history of the observations in Venice), a couple of hours later than
570 the astronomical tide maximum, then the RSL decreased to 119 cm at 16:35 UTC at rose again up to 148 cm at 19:25
571 UTC. The surge level peaked at 92 cm together with the maximum RSL and to 117 cm at 19:20 UTC, in coincidence
572 with the astronomical tide minimum. The 117 surge level represents the second highest ever observed and the 119 cm
573 value the highest minimum RSL. Overall, the RSL was higher than 120 cm for 14 hr, as on 4 November 1966.

574 **A1.9 12, 15 and 17 November 2019**

575 On November 12th, 2019, an exceptional flood event took place in Venice, second only to the one that occurred on
576 November 4th, 1966. Moreover, with 15 high tides higher than 110 cm and 4 events above 140 cm, November 2019 was
577 the worst month for flooding in Venice since the beginning of sea-level records.

578 The extreme high sea level recorded in Venice was due to the combination of the following large-scale and local
579 dynamics: the in-phase timing between the peak of the atmospheric surge and the lower high astronomical tide; a standing
580 low-pressure and wind systems over the Mediterranean Sea - that is associated with planetary atmospheric waves trough
581 extending over the whole month of November - which determined a high monthly mean sea level in the northern Adriatic
582 Sea; a deep low-pressure system over the central-southern Tyrrhenian Sea that generated south-easterly winds along the
583 main axis of the Adriatic Sea, pushing waters to the north; a fast-moving local cyclone travelling in the north-westward
584 direction over the Adriatic Sea along the Italian coast, generating a meteotsunami; very strong south-westerly winds over
585 the Lagoon of Venice, which led to a rise in water levels and damages to the historic city.

586 The SLP minimum of the cyclone on the Tyrrhenian Sea was about 990 hPa. A small deep secondary SLP minimum
587 formed in the afternoon, reaching 988 hPa at Venice around 21 UTC. Initially, moderate northeasterly wind was blowing
588 over the north Adriatic (about 10 m s^{-1} at Venice), but between 21 and 22 UTC it veered to S,E then to SW, and sustained
589 wind reinforced up to 20 m s^{-1} at Tessera airport.

590 The highest RSL was reached at 21:50 UTC with 189 cm, that represents the second highest value in the history of the
591 observations in Venice, and it almost exactly coincided with the astronomical tide peak. The surge level peaked at 100
592 cm, representing the fourth highest value ever observed. The peak RSL was similar to the 1966 value (namely 194 cm),
593 but, while in 1966 it was mainly the result of a huge meteorological component (143 cm, see A1.3 above), in 2019 the
594 astronomical tide contribution also played a significant role. Moreover, in 2019 the relative sea level was 11 cm higher
595 with respect to 1966.

596 On 15 November another storm surge developed in connection with a large cyclone over west Europe, having a 995 hPa
597 SLP minimum over France, and extending into Algeria. Local pressure in Venice reached 1001 hPa and wind blew from
598 SE at less than 10 m s^{-1} . The RSL peaked at 154 cm at 10:40 UTC and the surge peak occurred 6.5 hours later with 62
599 cm.

600 **Appendix II: A note on cyclone tracking algorithm**

601 Cyclones producing extreme surges have been identified and tracked using a cyclone detection and tracking method
602 applied to the gridded ERA5 mean sea-level pressure (SLP) fields with a spatial resolution of 0.25° and a temporal



603 resolution of 6 h. This dataset covers the period 1979–2018. The cyclone detection and tracking has been extensively
604 described in previous studies (Lionello, Dalan et al. 2002, Reale and Lionello 2013, Lionello, Trigo et al. 2016). It is
605 based on the search of pressure minima in MSLP-gridded fields. It identifies the location where each cyclogenesis process
606 occurs and constructs the trajectory of the pressure minimum by joining the location of the low-pressure centre in
607 successive maps until it disappears (cyclolysis). This cyclone tracking algorithm contains features that are meant to detect
608 the formation of cyclones inside the Mediterranean and, at the same time, avoid the inflation of the number of cyclones,
609 determined by considering small, short-lived features as independent systems. The method first partitions the sea-level
610 pressure (SLP) field in depressions, which can be considered candidates for independent cyclones, by merging all steepest
611 descent paths leading to the same minimum.

612

613 **Appendix III Wavelet of the storm surge frequency**

614 In order to integrate the discussion in section 5.3 on the presence of a 11-year periodicity of storm surges, Figures A.1
615 and A.2 show the amplitude of the wavelets of the autumn mean time series of Relative Sea Level (RSL) for 1924-2018
616 and of its daily extremes. In both graphics, a decadal signal consistent with the 11-year solar cycle is present only for a
617 few decades from the 1970s to the 1990s and absent before and after this period.

618

619

620 **References**

621

622 Androulidakis, Y. S., Kombiadou, K. D., Makris, C. V., Baltikas, V. N. and Krestenitis, Y. N. (2015) 'Storm surges in
623 the Mediterranean Sea: Variability and trends under future climatic conditions', *Dynamics of Atmospheres and Oceans*,
624 71, pp. 56-82.

625 Bajo, M., Medugorac, I., Umgiesser, G. and Orlić, M. (2019) 'Storm surge and seiche modelling in the Adriatic Sea and
626 the impact of data assimilation', *Quarterly Journal of the Royal Meteorological Society*, 145(722), pp. 2070-2084.

627 Bamber, J. L. and Aspinall, W. P. (2013) 'An expert judgement assessment of future sea-level rise from the ice sheets',
628 *Nature Climate Change*, 3(4), pp. 424-427.

629 Bargagli, A., Carillo, A., Pisacane, G., Ruti, P. M., Struglia, M. V. and Tartaglione, N. (2002) 'An Integrated Forecast
630 System over the Mediterranean Basin: Extreme Surge Prediction in the Northern Adriatic Sea', *Monthly Weather
631 Review*, 130(5), pp. 1317-1332.

632 Barriopedro, D., García-Herrera, R., Lionello, P. and Pino, C. (2010) 'A discussion of the links between solar variability
633 and high-storm-surge events in Venice', *Journal of Geophysical Research Atmospheres*, 115(13).

634 Battistin, D. and Canestrelli, P. (2006) *1872-2004 La serie storica delle maree a Venezia*, Venice, Italy: Istituzione
635 Centro Previsioni e Segnalazioni Maree. Available at:
636 [https://www.comune.venezia.it/sites/default/files/publicCPSM2/pubblicazioni/La_serie_storica_delle_maree_a_Venezi
637 a_1872-2004_web_ridotto.pdf](https://www.comune.venezia.it/sites/default/files/publicCPSM2/pubblicazioni/La_serie_storica_delle_maree_a_Venezi_a_1872-2004_web_ridotto.pdf).

638 Bertotti, L., Bidlot, J.-R., Buizza, R., Cavaleri, L. and Janousek, M. (2011) 'Deterministic and ensemble-based
639 prediction of Adriatic Sea sirocco storms leading to 'acqua alta' in Venice', *Quarterly Journal of the Royal
640 Meteorological Society*, 137(659), pp. 1446-1466.

641 Bertotti, L. and Cavaleri, L. (1985) 'Coastal set-up and wave breaking', *Oceanologica acta*, 8(2), pp. 237-242.



- 642 Camuffo, D. and Sturaro, G. (2004) 'Use of proxy-documentary and instrumental data to assess the risk factors leading
643 to sea flooding in Venice', *Global and Planetary Change*, 40(1), pp. 93-103.
- 644 Canestrelli, P., Mandich, M., Pirazzoli, P. A. and Tomasin, A. (2001) *Wind, Depressions and Seiche: Tidal
645 Perturbations in Venice (1951-2000)*, Venice, Italy: Istituzione Centro Previsioni e Segnalazioni Maree. Available at:
646 https://www.comune.venezia.it/sites/default/files/publicCPSM2/pubblicazioni/Venti_depressioni_e_sesse.pdf.
- 647 Caporin, M. and Fontini, F. (2016) 'Damages Evaluation, Periodic Floods, and Local Sea Level Rise: The Case of
648 Venice, Italy', *Handbook of Environmental and Sustainable Finance*: Elsevier, pp. 93-110.
- 649 Cavaleri, L., Bajo, M., Barbariol, F., Bastianini, M., Benetazzo, A., Bertotti, L., Chiggiato, J., Ferrarin, C., Trincardi, F.
650 and Umgiesser, G. (2020) 'The 2019 Flooding of Venice AND ITS IMPLICATIONS FOR FUTURE PREDICTIONS',
651 *Oceanography*, 33(1), pp. 42-49.
- 652 Cavaleri, L., Bertotti, L., Buizza, R., Buzzi, A., Masato, V., Umgiesser, G. and Zampieri, M. (2010) 'Predictability of
653 extreme meteo-oceanographic events in the Adriatic Sea', *Quarterly Journal of the Royal Meteorological Society*,
654 136(647), pp. 400-413.
- 655 Cerovečki, I., Orlić, M. and Hendershott, M. C. (1997) 'Adriatic seiche decay and energy loss to the Mediterranean',
656 *Deep Sea Research Part I: Oceanographic Research Papers*, 44(12), pp. 2007-2029.
- 657 Chiodo, G., Oehrlin, J., Polvani, L. M., Fyfe, J. C. and Smith, A. K. (2019) 'Insignificant influence of the 11-year solar
658 cycle on the North Atlantic Oscillation', *Nature Geoscience*, 12(2), pp. 94-99.
- 659 Codiga, D. L. (2011) *Unified tidal analysis and prediction using the UTide Matlab functions*. Graduate School of
660 Oceanography, University of Rhode Island Narragansett, RI.
- 661 Conte, D. and Lionello, P. (2013) 'Characteristics of large positive and negative surges in the Mediterranean Sea and
662 their attenuation in future climate scenarios', *Global and Planetary Change*, 111, pp. 159-173.
- 663 De Zolt, S., Lionello, P., Nuhu, A. and Tomasin, A. (2006) 'The disastrous storm of 4 November 1966 on Italy', *Natural
664 Hazards and Earth System Science*, 6(5), pp. 861-879.
- 665 Dorigo, L. (1961a) *Le osservazioni mareografiche in Laguna di Venezia*, Venice, Italy: Istituto Veneto di Scienze,
666 Lettere e Arti.
- 667 Dorigo, L. (1961b) *Maree eccezionali registrate a Venezia Punta della Salute. Periodo 1867-1960*: Istituto Veneto di
668 Scienze, Lettere e Arti.
- 669 Enzi, S. and Camuffo, D. (1995) 'Documentary sources of the sea surges in Venice from ad 787 to 1867', *Natural
670 Hazards*, 12(3), pp. 225-287.
- 671 Fagherazzi, S., Fossier, G., D'Alpaos, L. and D'Odorico, P. (2005) 'Climatic oscillations influence the flooding of
672 Venice', *Geophysical Research Letters*, 32(19).
- 673 Ferrarin, C., Maicu, F. and Umgiesser, G. (2017) 'The effect of lagoons on Adriatic Sea tidal dynamics', *Ocean
674 Modelling*, 119, pp. 57-71.
- 675 Ferrarin, C., Tomasin, A., Bajo, M., Petrizzo, A. and Umgiesser, G. (2015) 'Tidal changes in a heavily modified coastal
676 wetland', *Continental Shelf Research*, 101, pp. 22-33.



- 677 Ferrarin, C., Bajo, M., Benetazzo, A., Cavalari, L., Chiggiato, J., Davison, S., Davolio, S., Lionello, P., Orlić, M.,
678 Umgieser, G. (2020b). “Local and large-scale controls of the exceptional Venice floods of November 2019”, submitted
679 to *Progress in Oceanography*.
- 680 Franco, P., jeftić, L., Malanotte Rizzoli, P., Orlić, M. and Purga, N. (1982) 'Descriptive Model of the Northern
681 Adriatic', *Oceanologica Acta*, 5(3), pp. 11.
- 682 Garrido-Perez, J. M., Ordóñez, C., Barriopedro, D., García-Herrera, R. and Paredes, D. (2020) 'Impact of weather
683 regimes on wind power variability in western Europe', *Applied Energy*, 264, pp. 114731.
- 684 Hendershott, M. C. and Speranza, A. (1971) 'Co-oscillating tides in long, narrow bays; the Taylor problem revisited',
685 *Deep Sea Research and Oceanographic Abstracts*, 18(10), pp. 959-980.
- 686 Hersbach, H., Bell, B., Berrisford, P., Hirahara, S., Horányi, A., Muñoz-Sabater, J., Nicolas, J., Peubey, C., Radu, R.
687 and Schepers, D. (2020) 'The ERA5 global reanalysis', *Quarterly Journal of the Royal Meteorological Society*,
688 146(730), pp. 1999-2049.
- 689 ISPRA, C. a. and CNR-ISMAR (2020) *Un mese di alte maree eccezionali. Dinamica e anomalia dell'evento del 12*
690 *novembre 2019*. Available at: www.comune.venezia.it/content/le-acque-alte-eccezionali (Accessed: 30 September
691 2019).
- 692 Jackson, L. P. and Jevrejeva, S. (2016) 'A probabilistic approach to 21st century regional sea-level projections using
693 RCP and High-end scenarios', *Global and Planetary Change*, 146, pp. 179-189.
- 694 Janeković, I. and Kuzmić, M. (2005) 'Numerical simulation of the Adriatic Sea principal tidal constituents', *Ann.*
695 *Geophys.*, 23(10), pp. 3207-3218.
- 696 Jansa, A., Alpert, P., Buzzi, A. and Arbogast, P. (2001) 'MEDEX, cyclones that produce high impact weather in the
697 Mediterranean', Available at <http://medex.aemet.uib.es>.
- 698 Jevrejeva, S., Jackson, L. P., Riva, R. E. M., Grinsted, A. and Moore, J. C. (2016) 'Coastal sea level rise with warming
699 above 2 °C', *Proceedings of the National Academy of Sciences*, 113(47), pp. 13342-13347.
- 700 Jordà, G., Gomis, D. and Marcos, M. (2012) 'Comment on “Storm surge frequency reduction in Venice under climate
701 change” by Troccoli et al', *Climatic change*, 113(3-4), pp. 1081-1087.
- 702 Karabeg, M. and Orlić, M. (1982) 'The influence of air pressure on sea level in the North Adriatic—a frequency-domain
703 approach', *Acta Adriatica*, 23(1/2), pp. 21-27.
- 704 Lionello, P. (1995) 'Oceanographic prediction for the Venetian Littoral', *NUOVO CIMENTO DELLA SOCIETA*
705 *ITALIANA DI FISICA C-GEOPHYSICS AND SPACE PHYSICS*, 18(3), pp. 245-268.
- 706 Lionello, P. (2005) 'Extreme storm surges in the gulf of venice: Present and future climate', *Flooding and*
707 *Environmental Challenges for Venice and its Lagoon: State of Knowledge.*, pp. 59-69.
- 708 Lionello, P., Abrantes, F., Congedi, L., Dulac, F., Gacic, M., Gomis, D., Goodess, C., Hoff, H., Kutiel, H., Luterbacher,
709 J., Planton, S., Reale, M., Schröder, K., Vittoria Struglia, M., Toreti, A., Tsimplis, M., Ulbrich, U. and Xoplaki, E.
710 (2012a) 'Introduction: Mediterranean climate-background information', *The Climate of the Mediterranean Region*, pp.
711 xxxv-xc.
- 712 Lionello, P., Bhend, J., Buzzi, A., Della-Marta, P. M., Krichak, S. O., Jansa, A., Maheras, P., Sanna, A., Trigo, I. F. and
713 Trigo, R. (2006a) 'Cyclones in the Mediterranean region: climatology and effects on the environment', *Developments in*
714 *earth and environmental sciences*: Elsevier, pp. 325-372.



- 715 Lionello, P., Bhend, J., Buzzi, A., Della-Marta, P. M., Krichak, S. O., Jansà, A., Maheras, P., Sanna, A., Trigo, I. F. and
716 Trigo, R. 2006b. Chapter 6 Cyclones in the Mediterranean region: Climatology and effects on the environment.
717 *Developments in Earth and Environmental Sciences*.
- 718 Lionello, P., Cavaleri, L., Nissen, K. M., Pino, C., Raicich, F. and Ulbrich, U. (2012b) 'Severe marine storms in the
719 Northern Adriatic: Characteristics and trends', *Physics and Chemistry of the Earth*, 40-41, pp. 93-105.
- 720 Lionello, P., Conte, D., Marzo, L. and Scarascia, L. (2017) 'The contrasting effect of increasing mean sea level and
721 decreasing storminess on the maximum water level during storms along the coast of the Mediterranean Sea in the mid
722 21st century', *Global and Planetary Change*, 151, pp. 80-91.
- 723 Lionello, P., Conte, D. and Reale, M. (2019) 'The effect of cyclones crossing the Mediterranean region on sea level
724 anomalies on the Mediterranean Sea coast', *Nat. Hazards Earth Syst. Sci.*, 19(7), pp. 1541-1564.
- 725 Lionello, P., Dalan, F. and Elvini, E. (2002) 'Cyclones in the Mediterranean region: the present and the doubled CO2
726 climate scenarios', *Climate Research*, 22(2), pp. 147-159.
- 727 Lionello, P., Galati, M. B. and Elvini, E. (2012) 'Extreme storm surge and wind wave climate scenario simulations at
728 the Venetian littoral', *Physics and Chemistry of the Earth*, 40-41, pp. 86-92.
- 729 Lionello, P., Mufato, R. and Tomasin, A. (2005) 'Sensitivity of free and forced oscillations of the Adriatic Sea to sea
730 level rise', *Climate Research*, 29(1), pp. 23-39.
- 731 Lionello, P., Nizzero, A. and Elvini, E. (2003) 'A procedure for estimating wind waves and storm-surge climate
732 scenarios in a regional basin: The Adriatic Sea case', *Climate Research*, 23(3), pp. 217-231.
- 733 Lionello, P., Trigo, I. F., Gil, V., Liberato, M. L. R., Nissen, K. M., Pinto, J. G., Raible, C. C., Reale, M., Tanzarella,
734 A., Trigo, R. M., Ulbrich, S. and Ulbrich, U. (2016) 'Objective climatology of cyclones in the Mediterranean region: A
735 consensus view among methods with different system identification and tracking criteria', *Tellus, Series A: Dynamic
736 Meteorology and Oceanography*, 68(1).
- 737 Lionello, P., Zampato, L., Malguzzi, P., Tomasin, A. and Bergamasco, A. (1998) 'On the correct surface stress for the
738 prediction of the wind wave field and the storm surge in the Northern Adriatic Sea', *Nuovo Cimento della Societa
739 Italiana di Fisica C*, 21(5), pp. 515-532.
- 740 Lionello, P., Nicholls, J.R., Umgiesser, G., Zanchettin, D. (2020) 'Venice flooding and sea level: past evolution, present
741 issues and future projections' *Natural Hazards and Earth System Sciences (submitted)*
- 742 Livio, D. (1968) *Le alte maree eccezionali a Venezia*, Venice, Italy: Ufficio Idrografico del Magistrato alle Acque 156).
- 743 Malačič, V., Viezzoli, D. and Cushman-Roisin, B. (2000) 'Tidal dynamics in the northern Adriatic Sea', *Journal of
744 Geophysical Research: Oceans*, 105(C11), pp. 26265-26280.
- 745 Manca, B., Mosetti, F. and Zennaro, P. (1974) 'Analisi spettrale delle sesse dell'Adriatico.', *Bollettino di Geofisica
746 Teorica ed Applicata*, 16, pp. 10.
- 747 Marcos, M., Jordà, G., Gomis, D. and Pérez, B. (2011) 'Changes in storm surges in southern Europe from a regional
748 model under climate change scenarios', *Global and Planetary Change*, 77(3), pp. 116-128.
- 749 Martínez-Asensio, A., Marcos, M., Tsimplis, M. N., Gomis, D., Josey, S. and Jordà, G. (2014) 'Impact of the
750 atmospheric climate modes on Mediterranean sea level variability', *Global and Planetary Change*, 118, pp. 1-15.



- 751 Martínez-Asensio, A., Tsimplis, M. N. and Calafat, F. M. (2016) 'Decadal variability of European sea level extremes in
752 relation to the solar activity', *Geophysical Research Letters*, 43(22), pp. 11,744-11,750.
- 753 Mel, R., Carniello, L. and D'Alpaos, L. (2019) 'Dataset of wind setup in a regulated Venice lagoon', *Data in brief*, 26,
754 pp. 104386.
- 755 Mel, R., Sterl, A. and Lionello, P. (2013) 'High resolution climate projection of storm surge at the Venetian coast',
756 *Natural Hazards and Earth System Science*, 13(4), pp. 1135-1142.
- 757 Mentaschi, L., Vousdoukas, M., Voukouvalas, E., Sartini, L., Feyen, L., Besio, G. and Alfieri, L. (2016) 'The
758 transformed-stationary approach: a generic and simplified methodology for non-stationary extreme value analysis',
759 *Hydrol. Earth Syst. Sci.*, 20(9), pp. 3527-3547.
- 760 Mentaschi, L., Vousdoukas, M. I., Voukouvalas, E., Dosio, A. and Feyen, L. (2017) 'Global changes of extreme coastal
761 wave energy fluxes triggered by intensified teleconnection patterns', *Geophysical Research Letters*, 44(5), pp. 2416-
762 2426.
- 763 Međugorac, I., Orlić, M., Janeković, I., Pasarić, Z. and Pasarić, M. (2018) 'Adriatic storm surges and related cross-basin
764 sea-level slope', *Journal of Marine Systems*, 181, pp. 79-90.
- 765 Međugorac, I., Pasarić, M. and Orlić, M. (2016) 'Two recent storm-surge episodes in the Adriatic', *International
766 Journal of Safety and Security Engineering*, 6, pp. 8.
- 767 Neu, U., Akperov, M. G., Bellenbaum, N., Benestad, R., Blender, R., Caballero, R., Coccozza, A., Dacre, H. F., Feng,
768 Y., Fraedrich, K., Grieger, J., Gulev, S., Hanley, J., Hewson, T., Inatsu, M., Keay, K., Kew, S. F., Kindem, I.,
769 Leckebusch, G. C., Liberato, M. L. R., Lionello, P., Mokhov, I. I., Pinto, J. G., Raible, C. C., Reale, M., Rudeva, I.,
770 Schuster, M., Simmonds, I., Sinclair, M., Sprenger, M., Tilinina, N. D., Trigo, I. F., Ulbrich, S., Ulbrich, U., Wang, X.
771 L. and Wernli, H. (2013) 'Imilast: A community effort to intercompare extratropical cyclone detection and tracking
772 algorithms', *Bulletin of the American Meteorological Society*, 94(4), pp. 529-547.
- 773 Oppenheimer, M., Glavovic, B., Hinkel, J., Van de Wal, R., Magnan, A. K., Abd-Elgawad, A., Cai, R., Cifuentes-Jara,
774 M., Deconto, R. M. and Ghosh, T. 2019. Sea level rise and implications for low-lying islands, coasts and communities
775 IPCC Special Report on the Ocean and Cryosphere in a Changing Climate ed HO Pörtner et al.
- 776 Orlić, M. (2001) 'Anatomy of sea level variability-an example from the Adriatic', *The Ocean Engineering Handbook*:
777 CRC Press.
- 778 Pasarić, M. and Orlić, M. (2001) 'Long-term meteorological preconditioning of the North Adriatic coastal floods',
779 *Continental Shelf Research*, 21(3), pp. 263-278.
- 780 Pirazzoli, P. A. and Alberto, T. (2002) 'Recent Evolution of Surge-Related Events in the Northern Adriatic Area',
781 *Journal of Coastal Research*, 18(3), pp. 537-554.
- 782 Raicich, F. (2015) 'Long-term variability of storm surge frequency in the Venice Lagoon: an update thanks to 18th
783 century sea level observations', *Nat. Hazards Earth Syst. Sci.*, 15(3), pp. 527-535.
- 784 Reale, M., Liberato, M. L. R., Lionello, P., Pinto, J. G., Salon, S. and Ulbrich, S. (2019) 'A global climatology of
785 explosive cyclones using a multi-tracking approach', *Tellus A: Dynamic Meteorology and Oceanography*, 71(1), pp.
786 1611340.
- 787 Reale, M. and Lionello, P. (2013) 'Synoptic climatology of winter intense precipitation events along the Mediterranean
788 coasts', *Natural Hazards and Earth System Sciences*, 13(7), pp. 1707-1722.



- 789 Robinson, A. R., Tomasin, A. and Arregiani, A. (1973) 'FLOODING VENICE PHENOMENOLOGY AND
790 PREDICTION OF THE ADRIATIC STORM SURGE', *Quarterly Journal of the Royal Meteorological Society*, 99(422
791 (OCTOBER, 1973)), pp. 688-692.
- 792 Roland, A., Cucco, A., Ferrarin, C., Hsu, T.-W., Liau, J.-M., Ou, S.-H., Umgiesser, G. and Zanke, U. (2009) 'On the
793 development and verification of a 2-D coupled wave-current model on unstructured meshes', *Journal of Marine
794 Systems*, 78, pp. S244-S254.
- 795 Šepić, J., Vilibić, I. and Belušić, D. (2009) 'Source of the 2007 Ist meteotsunami (Adriatic Sea)', *Journal of Geophysical
796 Research: Oceans*, 114(C3).
- 797 Thiéblemont, R., Matthes, K., Omrani, N.-E., Kodera, K. and Hansen, F. (2015) 'Solar forcing synchronizes decadal
798 North Atlantic climate variability', *Nature Communications*, 6(1), pp. 8268.
- 799 Tomasin, A. (2002) *The frequency of Adriatic surges and solar activity*.: Istituto Studio Dinamica Grandi Masse
800 (ISDGM-CNR).
- 801 Toretì, A., Xoplaki, E., Maraun, D., Kuglitsch, F.-G., Wanner, H. and Luterbacher, J. (2010) 'Characterisation of
802 extreme winter precipitation in Mediterranean coastal sites and associated anomalous atmospheric circulation patterns',
803 *Natural Hazards and Earth System Sciences*, 10(5), pp. 1037-1050.
- 804 Trigo, I. F., Bigg, G. R. and Davies, T. D. (2002) 'Climatology of Cyclogenesis Mechanisms in the Mediterranean',
805 *Monthly Weather Review*, 130(3), pp. 549-569.
- 806 Trigo, I. F. and Davies, T. D. (2002) 'Meteorological conditions associated with sea surges in Venice: a 40 year
807 climatology', *International Journal of Climatology*, 22(7), pp. 787-803.
- 808 Trigo, I. F., Davies, T. D. and Bigg, G. R. (1999) 'Objective climatology of cyclones in the Mediterranean region',
809 *Journal of climate*, 12(6), pp. 1685-1696.
- 810 Troccoli, A., Zambon, F., Hodges, K. I. and Marani, M. (2012) 'Storm surge frequency reduction in Venice under
811 climate change', *Climatic change*, 113(3-4), pp. 1065-1079.
- 812 Ulbrich, U., Leckebusch, G. C., Grieger, J., Schuster, M., Akperov, M., Bardin, M. Y., Feng, Y., Gulev, S., Inatsu, M.,
813 Keay, K., Kew, S. F., Liberato, M. L. R., Lionello, P., Mokhov, I. I., Neu, U., Pinto, J. G., Raible, C. C., Reale, M.,
814 Rudeva, I., Simmonds, I., Tilinina, N. D., Trigo, I. F., Ulbrich, S., Wang, X. L. and Wernli, H. (2013) 'Are Greenhouse
815 Gas Signals of Northern Hemisphere winter extra-tropical cyclone activity dependent on the identification and tracking
816 algorithm?', *Meteorologische Zeitschrift*, 22(1), pp. 61-68.
- 817 Ulbrich, U., Leckebusch, G. C. and Pinto, J. G. (2009) 'Extra-tropical cyclones in the present and future climate: a
818 review', *Theoretical and Applied Climatology*, 96(1-2), pp. 117-131.
- 819 Ulbrich, U., Lionello, P., Belušić, D., Jacobeit, J., Knippertz, P., Kuglitsch, F. G., Leckebusch, G. C., Luterbacher, J.,
820 Maugeri, M., Maheras, P., Nissen, K. M., Pavan, V., Pinto, J. G., Saaroni, H., Seubert, S., Toretì, A., Xoplaki, E. and
821 Ziv, B. (2012) 'Climate of the mediterranean: Synoptic patterns, temperature, precipitation, winds, and their extremes',
822 *The Climate of the Mediterranean Region*, pp. 301-346.
- 823 Umgiesser, G., Canu, D. M., Cucco, A. and Solidoro, C. (2004) 'A finite element model for the Venice Lagoon.
824 Development, set up, calibration and validation', *Journal of Marine Systems*, 51(1-4), pp. 123-145.
- 825 Umgiesser, G. et al. (2020) The prediction of floods in Venice: methods, models and uncertainty", *Natural Hazards and
826 Earth System Sciences (submitted)*



- 827 Vilibić, I. and Šepić, J. (2009) 'Destructive meteotsunamis along the eastern Adriatic coast: Overview', *Physics and*
828 *Chemistry of the Earth, Parts A/B/C*, 34(17), pp. 904-917.
- 829 Vousdoukas, M. I., Mentaschi, L., Voukouvalas, E., Verlaan, M. and Feyen, L. (2017) 'Extreme sea levels on the rise
- 830 along Europe's coasts', *Earth's Future*, 5(3), pp. 304-323.
- 831 Vousdoukas, M. I., Mentaschi, L., Voukouvalas, E., Verlaan, M., Jevrejeva, S., Jackson, L. P. and Feyen, L. (2018)
- 832 'Global probabilistic projections of extreme sea levels show intensification of coastal flood hazard', *Nature*
- 833 *Communications*, 9(1), pp. 2360.
- 834 Vousdoukas, M. I., Voukouvalas, E., Annunziato, A., Giardino, A. and Feyen, L. (2016) 'Projections of extreme storm
- 835 surge levels along Europe', *Climate Dynamics*, 47(9), pp. 3171-3190.
- 836 Zanchettin, D., Rubino, A., Traverso, P. and Tomasino, M. (2009) 'Teleconnections force interannual-to-decadal tidal
- 837 variability in the Lagoon of Venice (northern Adriatic)', *Journal of Geophysical Research Atmospheres*, 114(7).
- 838 Zanchettin, D. et al. (2020) "Sea-level rise in Venice: historic and future trends", *Natural Hazards and Earth System*
- 839 *Sciences (submitted)*

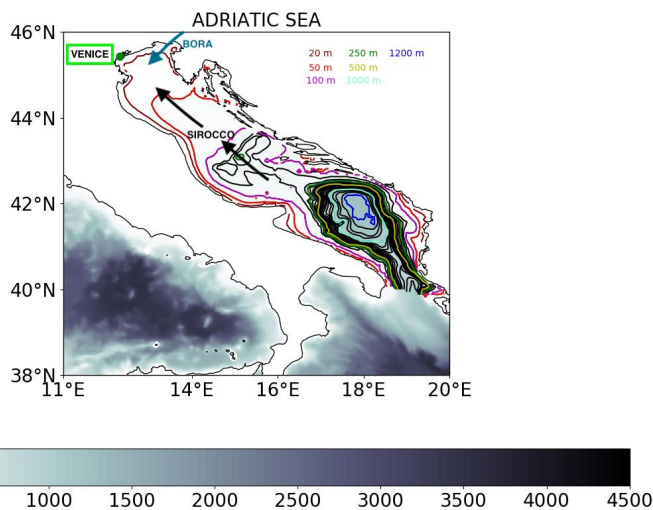
840

841

842

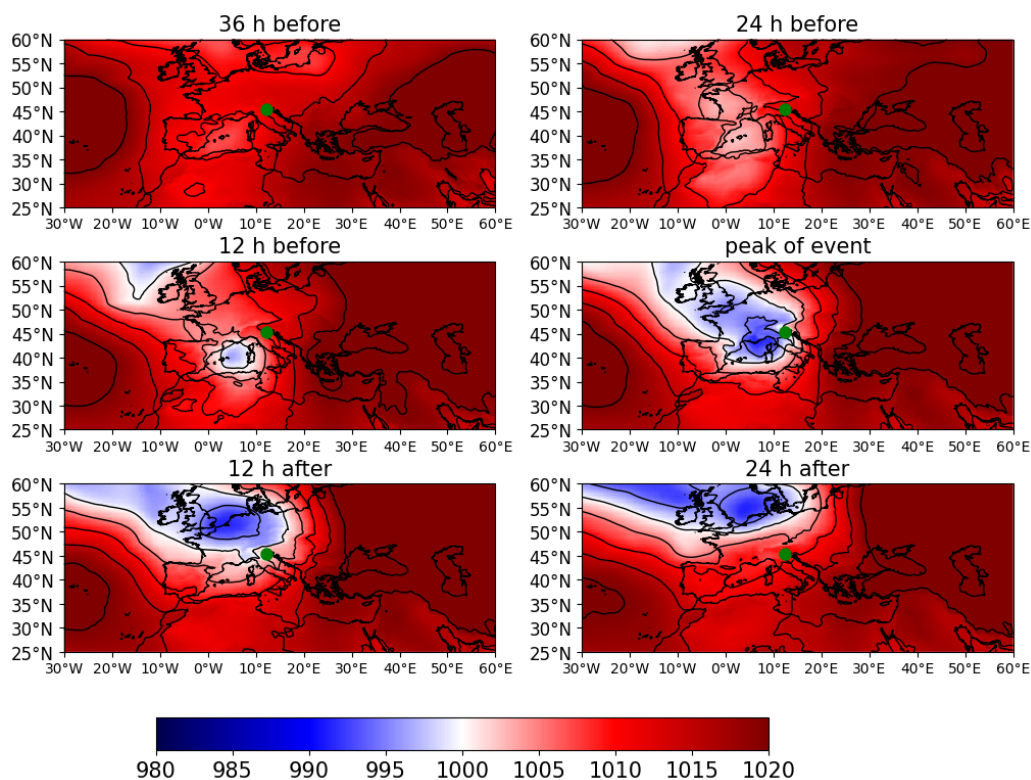
843

844



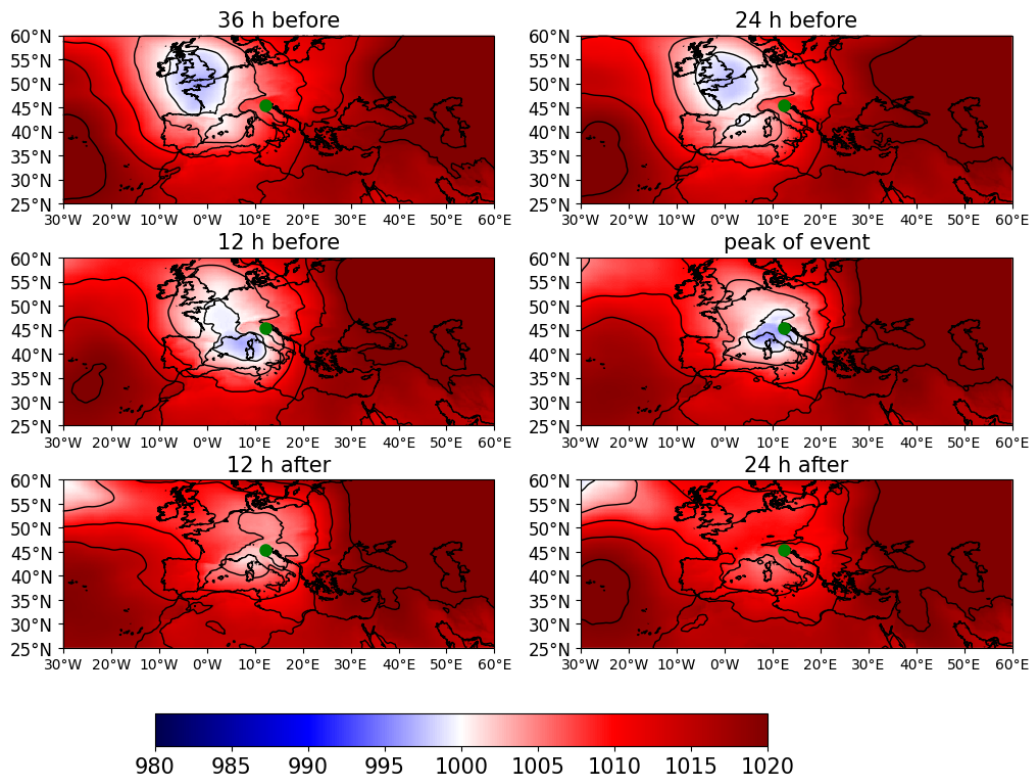
845

846 **Figure 1: Bathymetry of the Adriatic Sea with the position of Venice and arrows denoting the directions of the two main wind**
847 **regimes affecting the North Adriatic**



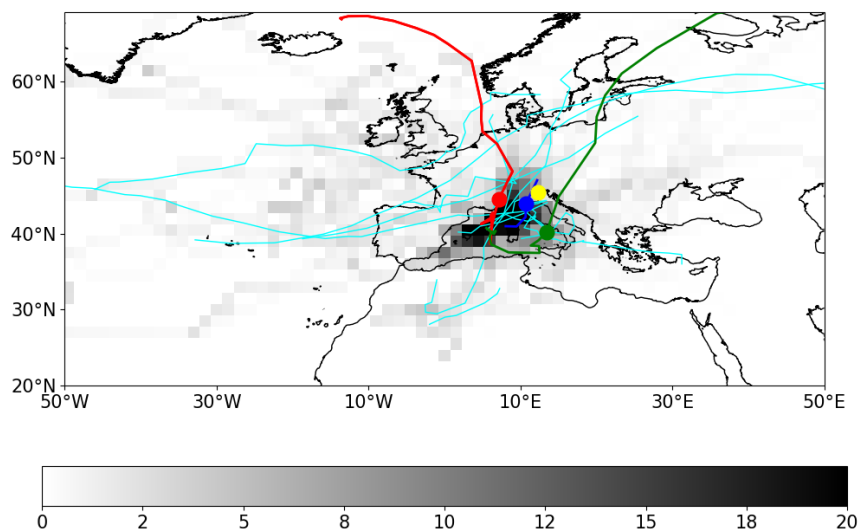
848

849 **Figure 2** Composite of SLP fields based on ERA5 (in hPa) datasets associated with storm surges higher than 50 cm in Venice
850 (see table 1). The time lags chosen for the composites is 36, 24, 12 hours before and 12, 24 hours after the peak of the event.
851 Green dot shows the location of the city of Venice



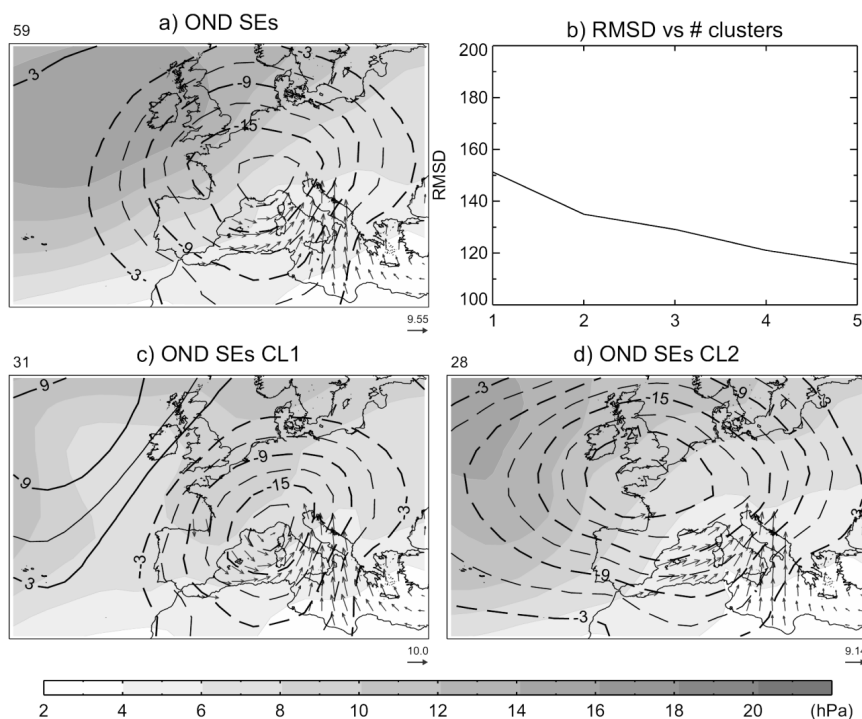
852

853 **Figure 3** Same as figure 2, except it is based on the events in table 1 with storm surge height lower than 50cm



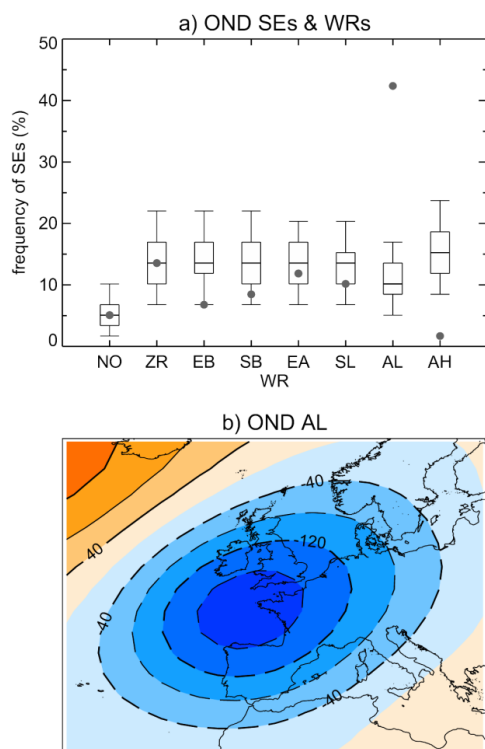
854
855 **Figure 4** Density of tracks of cyclones (contour, measured as relative frequency of cyclones for each cell of 1.5 in%) based on
856 ERA5 associated with storm surges with relative sea level higher than 110 cm . Cyan tracks represent the events reported in
857 Table 1 with relative sea level higher than 140 cm (see Table 1), red track is the track of Storm Vaia (2018, see Table 1) , green
858 line is the track of the event of November 2019. Blue line is the track of cyclone producing the event of 4 November 1966 (based
859 on ERA40 field). Yellow dot represents the location of the city of Venice while the blu, red and green dot represent the location
860 of the storm of 4 November 1996, storm Vaia (29/10/2018) and that one associated with the event of November 2019.
861

862



863

864 **Figure 5a)** Composite of daily anomalies of sea level pressure (SLP) over $[30,60]^{\circ}\text{N}$, $[30^{\circ}\text{W},30^{\circ}\text{E}]$ (contours, hPa) and 10 m
865 wind vector over the Mediterranean sea (arrows, m s⁻¹) for autumn surge events in Venice with surge height above the 99.5th
866 percentile of the 1948-2018 distribution. Shading shows the standard deviation of the composited SLP fields. The number of
867 cases is shown in the top left corner. The modulus of a reference wind speed vector is shown in the bottom right; b) Root mean
868 squared difference (RMSD) of the daily standardized anomalies of SLP and 10 m wind vector as a function of the number of
869 clusters. RMSDs are computed with respect to the centroid of the respective cluster; c, d) As a) but when surge events are split
870 in two groups, referred to as cluster one (CL1) and two (CL2), which correspond to the choice of two clusters in b). Note that
871 a) is equivalent to considering one cluster with all events. Data sources: NCEP/NCAR reanalysis (Kalnay et al. 1996) and Fabio
872 Raicich (Raicich 2015)

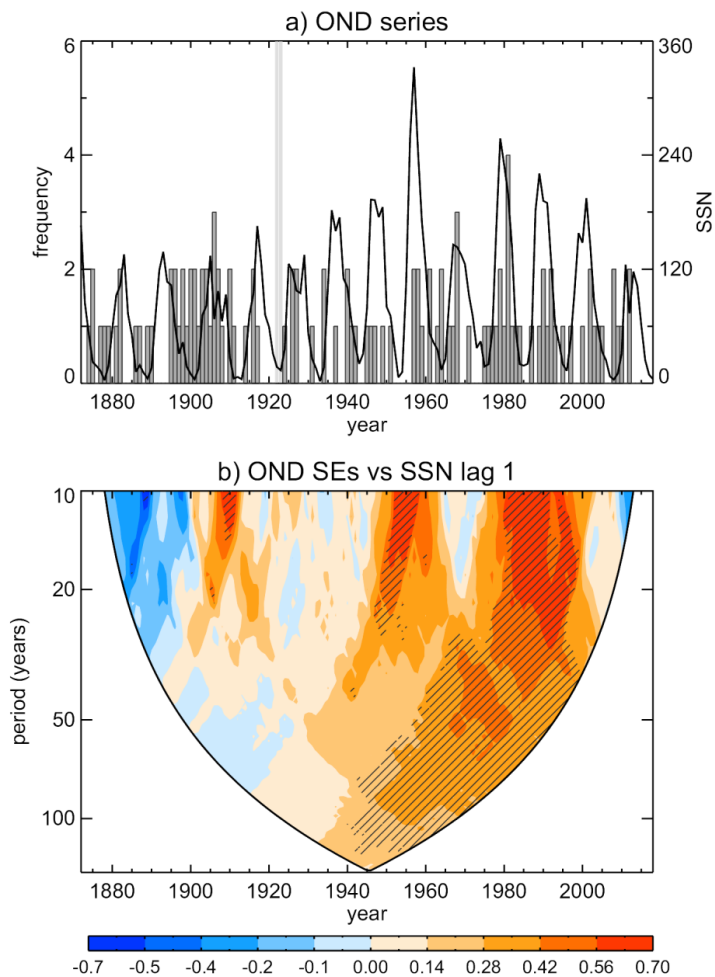


873

874 **Figure 6 . Top panel: Relative frequency of autumn extreme surge events in Venice for 1948-2018 (in % with respect to the**
875 **total number of events) occurring under the given Weather Regime (WR). Whiskers denote the random distributions obtained**
876 **from a bootstrap of 5000 trials, each one containing the same number of autumn days of the 1948-2018 period as surge events.**
877 **Boxes denote the inter-quartile distribution, with the median in between, and bars extend from the 5th to the 95th percentile**
878 **of the random distributions. Surge events are defined as those with surge height above the 99.5th percentile of the 1948-2018**
879 **distribution. WRs are defined from daily fields of geopotential height at 500 hPa of the NCEP/NCAR reanalysis over the Euro-**
880 **Atlantic sector [30, 65°N, [30°W, 25°E]. Acronyms stand for: NO: No (i.e. undefined) WR; ZR: Zonal Regime; EB: European**
881 **Blocking; SB: Scandinavian Blocking; EA: East Atlantic; SL: Scandinavian Low; AL: Atlantic Low; AH: Atlantic High. See**
882 **Garrido-Pérez et al. (2019) for further details. Bottom panel: The AL pattern which is associated to the occurrence of more**
883 **than 40% of extreme surges. Data sources: NCEP/NCAR reanalysis (Kalnay et al. 1996) and Fabio Raicich (Raicich 2015).**

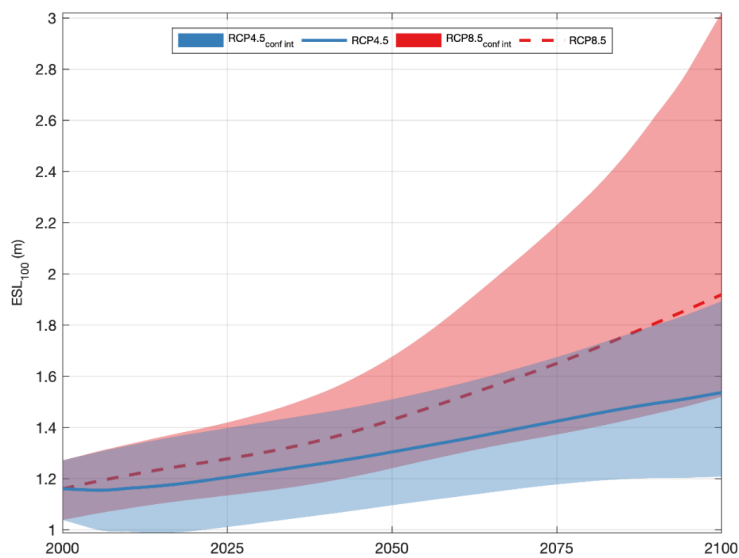


884



885

886 **Figure 7 top panel:** Time series of the autumn frequency of independent RSL extremes (SEs) for 1924-2018,
887 defined as daily peaks above the 99.5th percentile (35.0 cm) of the distribution formed by the RSL values of all-
888 year days of 1924-2018. Daily peaks are required to be separated by more than 72h. Black line shows the autumn
889 mean time series of the SunSpot Number (SSN). Bottom panel: Rank Spearman's (ρ) correlations between the
890 autumn frequency of surge events in Venice and the recently revised Sunspot Number (SSN) for running windows
891 of different width (y-axis) centered at each year of the 1872-2018 period (x-axis). Hatching denotes statistically
892 significant correlations ($p < 0.05$). Correlations are only computed when the sample size is equal or larger than 10
893 and it exceeds the half size of the window. The correlation pattern maximizes for SSN leading by 1-yr. Data
894 sources: WDC-SILSO, Royal Observatory of Belgium, Brussels (see Clette et al. 2014) and Raicich 2015)



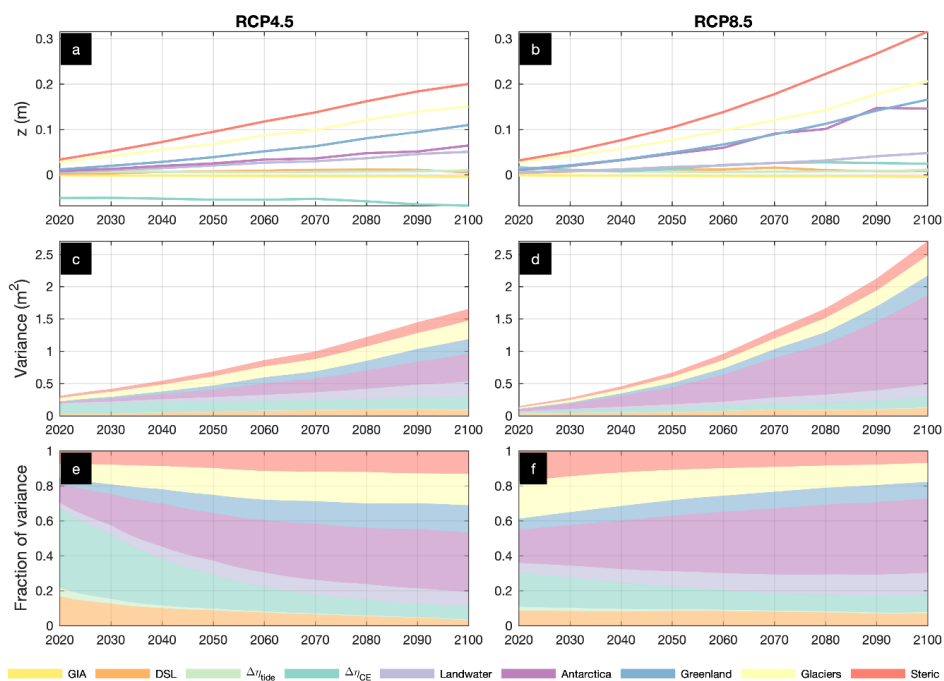
895

896 **Figure 8 Time evolution of the 100y-ESL: Time series of the 100y-ESL under RCP4.5 (blue) and RCP8.5 (red).**
897 **Heavy: median, patches express the 5th-95th percentiles (very likely range).**

898



899



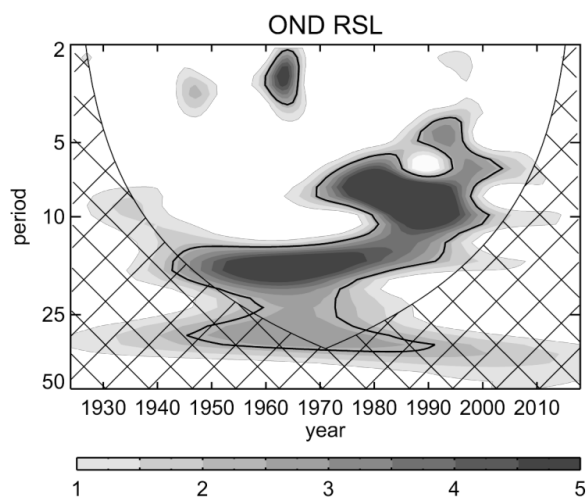
900

901 **Figure 9** Break-down of projected 100y-ESL contributions and of their uncertainty, under RCP4.5 (a, c, e) and
902 RCP8.5 (b, d, f). Projected increase of the 100y-ESL from changes in climate extremes, the high tide water level,
903 as well as from SLR contributions from Antarctica, land-water, Greenland, glaciers, dynamic sea level (DSL),
904 glacial isostatic adjustment (GIA), and steric-effects (a, b); variance (in m²) in components (c, d) and fraction of
905 components' variance in global 100y-ESL change. Colors represent different components as in the legend and
906 values express the global mean of the median.

907



908

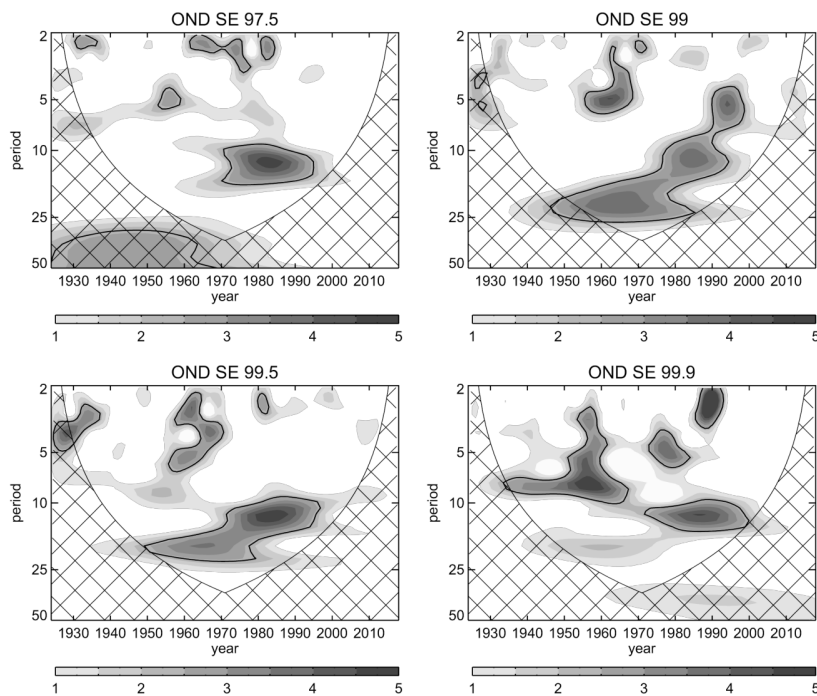


909

910 **Figure A.1** Wavelet of the autumn mean time series of Relative Sea Level (RSL) for 1924-2018, expressed as power
911 values normalized by the variance. Seasonal values are obtained from monthly means of the daily series. All
912 months of this period have less than 10% missing days. Significant power density at 90% confidence level is
913 highlighted by contours

914

915



916

917

918 **Figure A.2** As figure III.1 but for the autumn frequency series of independent SEs above the 97.5th, 99th , 99.5th and 99.9th
919 percentiles.



920
 921

Datetime [UTC]	RSL	Tide	Seiche	Storm surge	Meteotsunami + local setup	PAW surge	IDAS	Mean SL (10y running mean)
1966-11-04 17:00:00	194	-10	22	108	16	19	19	20
2019-11-12 21:50:00	189	36	5	43	38	20	15	32
1979-12-22 08:10:00	166	17	15	80	16	13	4	21
1986-02-01 03:00:00	159	31	23	48	4	18	13	22
2018-10-29 13:40:00	156	23	3	51	12	29	7	31
2008-12-01 09:45:00	156	39	22	43	0	18	5	29
2019-11-15 10:35:00	154	46	5	25	2	27	17	32
1951-11-12 07:05:00	151	45	1	43	2	39	5	16
2019-11-17 12:10:00	150	33	0	35	10	23	17	32
2012-11-11 08:25:00	149	50	-5	62	2	1	9	30
2018-10-29 19:25:00	148	-31	24	73	14	30	7	31
2002-11-16 08:45:00	147	40	-7	48	2	22	15	27
1936-04-16 20:35:00	147	20	15	60	7	27	7	11
2009-12-25 03:00:00	145	31	23	22	3	19	18	29
1960-10-15 06:55:00	145	33	4	63	2	11	14	18
2019-11-13 08:30:00	144	48	4	14	6	23	17	32
2010-12-24 00:40:00	144	36	1	37	4	22	14	30
2000-11-06 19:35:00	144	13	7	71	0	18	9	26
1968-11-03 06:30:00	144	43	10	43	2	18	7	21
2013-02-11 23:05:00	143	38	15	39	0	6	15	30
2012-11-01 00:40:00	143	16	3	54	3	27	10	30
2009-12-23 04:05:00	143	21	32	23	4	17	17	29
1992-12-08 09:10:00	142	43	6	31	2	35	1	24
1979-02-17 00:15:00	140	29	-3	39	10	27	17	21

922
 923
 924
 925

Table 1 List of the extreme sea levels higher than 140 cm alongside the contributions (see section 2.1 and 2.2): astronomical tide, seiches, storm surge, meteotsunami and local set-up, PAW surge, IDAS variability, Relative Mean Sea Level. All values in cm. The Relative Mean Sea level anomaly refers to the ‘Zero Mareografico Punta Salute’ (ZMPS).

926
 927



Date	RSL (cm)	Sources of RSL height
4-Nov-66	194	DO68, CA01, BC06, CPSM
12-Nov-19	189	ISPRA, CA20, CPSM
22-Dec-79	166	CA01, BC06, CPSM
1-Feb-86	159	CA01, BC06, CPSM
29 Oct 2018*	156	BC06, ISPRA, CPSM, CA19
1-Dec-08	156	BC06, ISPRA, CPSM
12-Nov-51	151	DO61, CA01, BC06, CPSM
11-Nov-12	149	BC06, ISPRA, CPSM
29 Oct 2018*	148	BC06, ISPRA, CPSM
16-Nov-02	147	BC06, CPSM
16-Apr-36	147	DO61, BC06, CPSM
25-Dec-09	145	BC06, CPSM
15-Oct-60	145	DO61, CA01, BC06, CPSM
24-Dec-10	144	BC06, ISPRA, CPSM
23-Dec-09	144	BC06, CPSM
6-Nov-00	144	CA01, BC06, CPSM
3-Nov-68	144	CA01, BC06, CPSM
12-Feb-13	143	BC06, ISPRA, CPSM
1-Nov-12	143	BC06, ISPRA
8-Dec-92	142	CA01, BC06, CPSM

928

929 Table A.1 List of the surge events higher than 100 cm alongside the respective RSL. The asterisk indicates the two RSL peaks
 930 during the same event on 29 October 2018. (AN41 = Annali, 1941; CA01 = Canestrelli et al., 2001; CA19 = Cavaleri et al., 2019,
 931 CA20 = Cavaleri et al., 2020, CPSM = CPSM, 2020; DE06 = de Zolt et al., 2006; DO61 = Dorigo, 1961b; DO68 = Dorigo, 1968;
 932 ISPRA = ISPRA, 2008-2018; ISPRA/CPSM/CNR = ISPRA et al., 2020)